NASA TECHNICAL MEMORANDUM

NASA TM X-62,168

NASA TM X-62,168

STUDY OF BUOYANCY SYSTEMS FOR FLIGHT VEHICLES

C. Dewey Havill and Louis J. Williams

Office of Aeronautics and Space Technology
Advanced Concepts and Missions Division
Moffett Field, California 94035

NATIONAL AERONAUTICS AND SPACE ADMINISTRATION
WASHINGTON, D. C. DECEMBER 1972

SUMMARY

A study has been conducted to examine the performance potential of buoyant systems and flexible structures used in air vehicles for short-haul passenger transportation. No attempt was made to assess the unique design and operational problems associated with such systems. The study was intended only to determine if sufficient performance potential existed, and to provide a focus for a more extensive design study, if such a study appeared desirable. A relatively conventional helium system was examined along with a more unusual configuration employing hot-air as the buoyant fluid. Both configurations were examined in the VTOL and STOL modes of operation. The helium system appears to have some superiority in the VTOL mode, while the hot-air system has a superiority in the STOL mode. Both configurations exhibit sufficient performance potential to suggest that a much more extensive design study might well be undertaken.

INTRODUCTION

After several decades of relative inactivity, a renewed interest has arisen in buoyant flight systems. Proposed uses for such systems range from intra- or inter-city passenger transportation to heavy-weight long-range cargo carriers. Possible advantages of such systems would be low power requirements, vertical takeoff, operational flexibility, and increased safety. Low power might be achieved because some fraction of the weight is supported with buoyant lift instead of aerodynamic lift. Implicit in low power are decreased operational noise, decreased air pollution, and possibly decreased costs. Helicopters have demonstrated the value of

vertical takeoff, but the value of operational flexibility cannot be properly assessed until a history of use is developed. Buoyant vehicles are not limited by land-sea interfaces, by bridge or road routes, or even by airports in a normal sense. In some applications a landing would not even be required to discharge cargo. In the normal transportation of passengers and cargo, properly utilized buoyant systems could eliminate at least one transportation interface, reducing overall transportation costs. Also the variety of missions which a single design can effectively perform is far greater than for any other transportation system. Due to several dramatic and well publicized accidents which occurred before modern technology existed, buoyant systems have a public image of being unduly hazardous. Such an image is the opposite of reality, and such vehicles may become the safest mode of transportation ever developed. Their large size increases their visibility so greatly that the risk of in-flight collisions should be reduced; their low speeds on takeoff and landing minimize the source and severity of most aircraft accidents; and finally, given almost any system failure, such vehicles can still be brought gently to the earth's surface.

Because of the potential advantages, an exploratory study has been conducted to estimate the performance of a particular class of such vehicles. Its purpose was to determine whether a more extensive study was desired, and in that event, to establish a focal point for such a study. This preliminary study made no attempt to examine the unique design and operational problems associated with such systems, and thus does not present conclusions relating to their feasibility. It does provide results showing what performance might be expected for a variety of configurational and operational assumptions.

The study considers two basic configurations, one the Dynastat configuration from reference 1 consisting of a helium blimp shaped to provide good aerodynamic lift and sized to buoyantly lift only a portion of the vehicle total weight. Vertical takeoff would be achieved by rotation of the propulsion system thrust vector. The other configuration consisted of a parawing taken from reference 2. It was assumed to be double layered, with the space between layers inflated to provide buoyant lift for vertical takeoff. Both configurations were studied for VTOL and STOL applications, with buoyant systems sized to provide net buoyant lifts ranging from 0 to more than 90% of the vehicle weight. The assumed mission was transportation of a 35-passenger personnel compartment, sized in reference 3 for use with a tilt-rotor VTOL vehicle.

Theoretical estimates were developed for the aerodynamic characteristics of the Dynastat vehicle and are presented in Appendix A. Appendix B presents a mathematical development approximating sizing relationships for the parawing.

NOMENCLATURE

a,b	constants in thrust equation
a_o	ground acceleration - ft/sec^2 (m/sec^2)
C_{DC}	drag coefficient at cruise
C_{DO}	zero lift drag coefficient
C_f	useful fuel, percent
C_L	lift coefficient
C_{LC}	cruise lift coefficient
C_{LL}	landing lift coefficient

D_C	cruise drag - lbs (N)
D_O	takeoff drag - lbs (N)
f_1, f_2, f_3	functions in cruise velocity equation
F_C	cruise thrust - lbs (N)
F_O	takeoff thrust - lbs (N)
(F_o/P_o)	zero velocity thrust coefficient - lbs(N)/horsepower
g	acceleration of gravity - ft/sec^2 (m/s^2)
K	coefficient of drag due to lift
K_{BO}, K_{BCO}	buoyant system weight coefficient - lbs/ft^3 (kg/m^3)
K_E	engine weight coefficient
K_L	buoyant system length coefficient
K_{LNBO}	buoyant lift coefficient - lbs/ft^3 (N/m^3)
L	aerodynamic lift - lbs (N)
L_C	cruise aerodynamic lift - lbs (N)
$(L/D)_C$	cruise lift-drag ratio
L_{NBC}	cruise net buoyant lift - lbs (N)
L_{NBO}	takeoff net buoyant lift - lbs (N)
L_o	takeoff aerodynamic lift - lbs (N)
$(L/D)_o$	takeoff lift-drag ratio
P_C	cruise power - horsepower
P_O	rated power - horsepower
q_c	cruise dynamic pressure - lbs/ft^2 (N/m^2)
R	range - miles (km)
SFC	specific fuel consumption - lbs(kg)/horsepower sec
t_c	time at cruise - sec
t_o	takeoff time - sec
T_G	buoyant gas temperature - °Rankine (°K)

V_B	bucyant volume ft^3 (m^3)
v_c	cruise velocity - ft/sec (m/s)
v_L	landing speed - ft/sec (m/s)
W_B	weight of buoyancy system - lbs (kg)
W_E	propulsion system weight - lbs (kg)
W_f	fuel weight - lbs (kg)
W_{FD}	rate of fuel usage - lbs/sec (kg/sec)
W_g	vehicle gross weight - lbs (kg)
W_{PC}	personnel compartment weight - lbs (kg)
x_o	takeoff length - ft (m)
AC	air density at cruise altitude - slugs/ft^3 (kg/m^3)

CONFIGURATIONS

Dynastat

The first configuration examined was based on the buoyant system presented in the reference 1 Dynastat proposal. A drawing from reference 1 showing dimensional data for the vehicle is presented in figure 1. Buoyant system weight and lift coefficients were obtained from reference 1 data, while aerodynamic coefficients were derived as discussed in appendix A. The buoyant system size was varied over a wide range from 25,000 ft^3 (708 m^3) to over 700,000 ft^3 (19,820 m^3), with no assumed change in the weight and aerodynamic coefficients. The weight of a 35-passenger personnel compartment taken from reference 3 was assumed as the payload for the entire study. Aerodynamics of the payload were ignored, and would probably have little effect on the results for appreciable percentages of buoyant lift. However, significant error might be introduced by this assumption for the smaller buoyant volumes, and particularly for the STOL configurations.

For the VTOL studies, engine power was varied parametrically, with the remaining required vertical takeoff force supplied by properly sizing the buoyant system. Propulsion system characteristics at the takeoff and cruise conditions were obtained using mathematical approximations to performance curves given in reference 4 for shrouded propellors, propfans, and fans. Values obtained in this way are presented in table I. For the STOL studies, engines were sized to produce a thrust 25% greater than vehicle drag with the vehicle taking off at maximum lift coefficient.

A value of fuel weight was assumed at the outset and maintained for the entire study. The assumed value was rather arbitrary, but its only use was to obtain relative values of range for the various configurations and operating procedures, and thus obtain their relative efficiencies as flight vehicles.

Parawing

A shortcoming of buoyant systems which lift all or an appreciable portion of the vehicle weight, is their large surface area, and the corresponding high zero lift drag. This has a strong limiting effect on cruise velocities, for reasonable power levels. It was hypothesized that if the buoyant gas could be released following takeoff, and the buoyant volume collapsed, then even though the surface area is the same, a more efficient aerodynamic lifting area might be created, with an improvement in cruise potential. Such a system would use hot-air as the buoyant gas, since recompression and storage of helium, or its release to the atmosphere, both appear to be undesirable.

The cylindrically designed, 2.7 aspect ratio vehicle in reference 2 (fig. 1 b) was chosen to evaluate a flight deflatable buoyant system.

Its weight, volume, and aerodynamic characteristics are developed in Appendix B. There may be some severe design and operational problems associated with such a vehicle, and these were all ignored. In order to minimize the extent of this effort, it was simply assumed that such vehicles could be developed and operated, and the study was confined to evaluating their size, power, speed, range, and takeoff characteristics. In this way, the study was intended to determine whether or not such vehicles would be worthwhile if the various problems have practical solutions.

ANALYTICAL PROCEDURE

Vertical Takeoff and Landing

Evaluations of the two configurations sized for VTOL were made by assuming various levels of propulsive power, computing propulsive lift corresponding to these power levels, and sizing a buoyant system to provide the required takeoff lift which remained. From these two quantities, propulsive power and buoyant lift, cruise velocities at various assumed altitudes could be ascertained and used to compute vehicle range. The following paragraphs indicate the method by which the computations were performed, and the various assumptions which were necessary.

Performance and sizing calculations assumed vehicle weight separated into three components: weight of the personnel compartment, W_{PC}, power system weight, W_E, which included engine, installation, and thrustor weights, and fuel weights, W_f. It was not necessary to deal with buoyancy system weight directly, since net buoyant lift, which was used in the calculations, is that lift remaining after the buoyant system has lifted its own weight. The buoyant system was sized to produce 20% more net lift than that required to lift the sum of these weights reduced by the vertical takeoff thrust of the power system.

$$L_{NBO} = 1.2 (W_{PC} + W_E + W_f - F_O) \quad (1)$$

Propulsion system characteristics were obtained for various propulsors, using mathematical approximations to performance curves given in reference 4. The approximating relationships are as follows:

Sea level zero velocity thrust is

$$F_O = \left(\frac{F_O}{P_O}\right) P_O \quad (2)$$

where $\left(\frac{F_O}{P_O}\right)$ = constant obtained from reference 4 data

P_O = sea level zero velocity shaft horsepower

Shaft horsepower at cruise is

$$P_C = 1.11 P_O \left(\frac{\rho_{AC}}{.002377} - 0.1\right) \quad (3)$$

where ρ_{AC} = air density at cruise altitude.

Thrust at cruise is

$$F_C = \frac{P_C}{a + b v_c^2} \quad (4)$$

where a and b are constants from ref 4 data

v_c = cruise velocity

Approximations to the reference 4 data for a, b, $\left(\frac{F_o}{P_o}\right)$, and the engine weight coefficient are given in table I. The weight coefficient, K_E, was arbitrarily increased by 50% to account for controls and installation. It is defined by the equation

$$W_E = K_E F_O \quad (5)$$

Required buoyancy system volume is given by the equations

$$V_B = \frac{L_{NBO}}{(.0649 - K_{BO})} \qquad \text{for Dynastat} \qquad (6)$$

and

$$V_B = \frac{L_{NBO}}{.0765\ (1 - \frac{572}{T_G}) - K_{BO}} \qquad \text{for parawing} \qquad (7)$$

where

K_{BO} = buoyancy system weight/volume

T_G = hot-air temperature - ^oR

For the Dynastat configuration, it was assumed that gas pressure remained constant during flight, and therefore if the vehicle was designed for higher altitude flight, pressure differential across the wall would be greater and the required buoyancy system weight would increase. A linear relationship between K_{BO} and atmospheric pressure was assumed giving

$$K_{BO} = 6\ K_{BOO}\ (1 - 350.5\ \rho_{AC}) \qquad (8)$$

K_{BOO} was evaluated using reference 1 data which gave a value of K_{BO} for an altitude of 3000 feet.

For the parawing, the buoyancy system weight coefficient does not change with cruise altitude since buoyancy lift is only used for takeoff. However, it does change with gas temperature, assuming that insulation is required. It was arbitrarily assumed that buoyancy system weight doubled when temperature increased 1000^{o}F, that the increase with temperature was linear, and that the weight coefficient at 60^{o}F was equal to that of a Helium system at sea level. These assumptions give

$$K_{BO} = K_{BOO}\ (1 + \frac{T_G - 520}{1000}) \qquad (9)$$

where T_G = ^{o}Rankine

and K_{BOO} is the same as previously used.

Vehicle drag at the cruise condition is

$$D_C = q_c \, C_{DC} \, (V_B)^{2/3} \tag{10}$$

where q_c = dynamic pressure = $1/2 \, \rho_{AC} \, v_c^2$ and the drag coefficient

$$C_{DC} = C_{DO} + K \, C_{LC}^2 \tag{11}$$

is based on $(V_B)^{2/3}$. Values for the constants

$$C_{DO} = .0190 \quad K = .2874$$

are developed in Appendix A for the Dynastat configuration.

For the parawing, the values

$$C_{DO} = .059 \quad K = .048$$

are developed in Appendix B.

In order to compute cruise velocity, v_c, the remaining relationships which must be established are those for required aerodynamic lift at cruise, and available aerodynamic lift at cruise. The desired aerodynamic lift at cruise is

$$L_C = W_{PC} + W_E + W_f - L_{NBC} \tag{12}$$

where $$L_{NBC} = (32.174 \, \rho_{AC} - .0116 - K_{BO}) \, V_B \text{ for Dynastat} \tag{13}$$

and $$L_{NBC} = - K_{BO} \, V_B \text{ for parawing} \tag{14}$$

The available lift is

$$L_C = 1/2 \, \rho_{AC} \, v_c^2 \, C_{LC} \, (V_B)^{2/3} \tag{15}$$

Equating (12) and (15) and solving for C_{LC} gives

$$C_{LC} = \frac{W_{PC} + W_E + W_f - L_{NBC}}{1/2\ \rho_{AC}\ (V_B)^{2/3}}\ \left(\frac{1}{v_c^2}\right) \tag{16}$$

or

$$C_{LC} = \frac{f_1}{v_c^2} \tag{17}$$

where

$$f_1 = \frac{W_{PC} + W_E + W_f - L_{NBC}}{1/2\ \rho_{AC}\ (V_B)^{2/3}}$$

Substituting this C_{LC} in equation (11) for C_{DC} gives

$$C_{DC} = K\left[\frac{C_{DO}}{K} + \frac{f_1^2}{v_c^4}\right] \tag{18}$$

Equating cruise thrust, eq. (4), with cruise drag, eg. (10), gives

$$\frac{P_C}{a+b\ v_c^2} = 1/2\ \rho_{AC}\ v_c^2\ C_{DC}\ (V_B)^{2/3} \tag{19}$$

If eq. (3) is substituted for P_C, and eq. (18) for C_{DC}, then (19) reduces to

$$(bf_3)\ v_c^6 + (af_3)\ v_c^4 + (bf_1^2 - f_2)\ v_c^2 + af_1^2 = 0 \tag{20}$$

where

$$f_2 = \frac{2.22\ P_0\ \left(\frac{\rho_{AC}}{.002377} - 0.1\right)}{K\ \rho_{AC}\ (V_B)^{2/3}}$$

$$f_3 = \frac{C_{DO}}{K}$$

Equation 20 was solved for v_c using a digital computer.

In addition to the quantities in the preceding equations, the following variables can be evaluated. Rate of fuel usage is

$$W_{FD} = (SFC)\ P_C$$

where SFC = specific fuel consumption, an input. Time at cruise is

$$t_c = \frac{C_f W_f}{W_{FD}}$$

where C_f = percentage of fuel used in cruise, an input. Cruise range is

$$R = \frac{v_c t_c}{5280} \text{ miles}$$

Lift drag ratio is

$$(L/D)_C = \frac{C_{LC}}{C_{DC}}$$

Weight of buoyant system is

$$W_B = K_{BO}\ V_B$$

Minimum landing speed is

$$v_L = \sqrt{\frac{f_1}{C_{LL}}}$$

where C_{LL} = maximum lift coefficient, an input.

Vehicle length is

$$L = K_L\ (V_B)^{1/3}$$

where K_L = configuration constant, an input.

= 2.974 for Dynastat

= 2.366 for parawing

Short Takeoff and Landing

If vertical takeoff is not required, then the sum of buoyant lift and propulsive thrust need not exceed vehicle weight. Therefore a buoyant system size can be assumed, and the propulsion system sized to produce sufficient thrust for horizontal takeoff. The following series of equations were used to perform this sizing.

$$W_B = .02872 \; V_B \tag{35}$$

Net buoyant lift

$$L_{NBO} = K_{LNBO} \; V_B \tag{36}$$

where K_{LNBO} is an assumed constant.

$$\text{Thrust } F_o = \frac{F_o}{P_o} \; P_o \tag{37}$$

where (F_o/P_o) is a propulsion system constant, and P_o is obtained through an iterative procedure. Engine weight, takeoff lift and takeoff drag are given by the following equations, respectively.

$$W_E = K_E \; F_o \tag{38}$$

$$L_o = W_{PC} + W_f - W_E - L_{NBO} \tag{39}$$

$$D_0 = \frac{L_o}{(L/D)_o} \tag{40}$$

where $(L/D)_o$ is obtained from the aerodynamic relationships presented previously, evaluated at the assumed maximum allowable lift coefficient.

An iteration is performed over equations (37)-(40), with an initial value of P_o assumed, and then increased during each iteration until the inequality exists

$$F_0 > 1.25 \; D_0$$

which is an assumed requirement.

Cruise conditions were established for a range of assumed cruise velocities, using the following series of relationships. Cruise aerodynamic lift is given by the force relationship

$$L_C = W_{PC} + W_E + W_f - L_{NBC} \tag{41}$$

where net buoyant lift at cruise is

$$L_{NBC} = (g \rho_{AC} - .0116 - K_{BO}) V_B \tag{42}$$

Cruise aerodynamic lift is also given by the aerodynamic equation

$$L_C = \frac{1}{2} \rho_{AC} V_C^2 C_{LC} V_B^{2/3} \tag{43}$$

which can be solved for cruise air density

$$\rho_{AC} = \frac{2 L_C}{V_C^2 C_{LC} V_B^{2/3}} \tag{44}$$

Substituting equations (44) and (42) into (41), and solving for cruise lift gives

$$L_C = \frac{(W_{PC} + W_E + W_f) + (.0116 + K_{BO}) V_B}{\frac{2 g V_B^{1/3}}{C_{LC} V_C^2} + 1} \tag{45a}$$

which is the value of cruise lift for the Dynastat configuration. Since the parawing configuration was assumed to contain precisely enough gas to support its own weight, the net buoyant lift is zero, and cruise lift becomes

$$L_C = W_{PC} + W_E + W_f \tag{45b}$$

Having obtained cruise lift, all other pertinent quantities can be obtained from the relationships presented in the VTOL phase of the study. When the value of cruise thrust is obtained, it is compared to cruise drag, and if less, a second iteration on P_o is made going back through equation (37). Therefore, the final value of engine power, and dependent quantities, satisfies both the takeoff and cruise requirements.

Required takeoff length is given by the equation

$$x_o = \frac{1}{2} a_o t_o^2 \tag{46}$$

where the ground acceleration is approximated by

$$a_o = \frac{g\,(F_o - \frac{1}{2} D_o)}{W_g} \tag{47}$$

and the time of acceleration is

$$t_o = \frac{V_o}{a_o} \tag{48}$$

RESULTS AND DISCUSSION

Vertical Takeoff and Landing

Results of the VTOL study are presented in figures 2 through 8. Data was obtained for cruise altitudes ranging from 3000 to 9000 ft (914 to 2743 m), for propellors, fans and prop-fans, and for percentages of propulsive lift ranging from about 10% to almost 100%. Figures 2, 3, and 4 present sea level shaft horsepower, buoyant volume, and buoyant system length, all as a function of propulsive lift at takeoff. Figure 2, for the Dynastat, indicates a distinct advantage, in power requirements, for propellers. Propellers providing 95% of the required takeoff lift require the same power as fans which only provide 25% of the takeoff lift. Buoyant system size is quite large, approaching 300 ft (91.4 m) in length as propulsive lift approaches zero, and remaining 100 ft (30.5 m) long even when supplying only 5% of the total takeoff lift. While there is a distinct increase in size with increased cruising altitude, the effect is relatively small. Figure 3 shows the same data for the parawing configuration, with the power requirements being identical since this parameter was not a function of buoyancy system configuration. The buoyancy system size characteristics in Figure 3 vary in the same fashion as for the Dynastat vehicle, and the factor of most significance is the relatively small sensitivity of size to gas temperature changes. This results from the increased buoyancy of higher temperature gas being partly offset by the additional weight of required insulation. Figure 4 presents a comparison of the Dynastat and parawing configurations at an altitude of 3000 ft (914 m), a hot-air gas temperature of 1500°R (833°K), and using propellers. As expected, the less efficient hot-air system required almost twice the volume, but due to its lower average fineness ratio, its overall length was slightly less than the helium system.

Performance data are presented in figures 5 through 8, which show cruise velocity, cruise range, and cruise lift-drag ratios as functions of propulsive lift. Figure 5 presents data at two altitudes for the three propulsor types, for the Dynastat configuration. Due to their larger takeoff power requirements, fan configurations indicate a higher cruising velocity. However, the difference in cruise velocity is insufficient to overcome the higher rate of fuel use, and their range is only 1/4 to 1/3 that of propellers. A change in cruise altitude from 3000 to 9000 ft (914 to 2743 m) generates a fairly substantial increase in lift-drag ratio, but this influence is not strongly reflected in either cruise velocity or cruise range. Cruise velocity shows a slight decrease with altitude, while cruise range shows a slight increase. It should be noted that a change in altitude affected propulsive thrust, net buoyant lift, and buoyancy system weight and size, as well as lift and drag coefficients, so no simple relationships can be assumed. Figures 6 and 7 present the same data for parawing vehicles with gas temperatures of 1250°R and 1500°R (694°K and 833°K), respectively. Differences between these two figures are very minor, indicating again the small influence of changes in gas temperature. Also again, the influence of large variations in lift-drag ratio are not reflected in velocity and range. A comparison of the performance parameters of the Dynastat and parawing vehicles is presented in figure 8. Both cruise velocity and cruise range were significantly inferior for the parawing vehicles, although for most of the data range they had a superior lift-drag ratio.

The initial reason for considering a hot-air system was to permit release of the buoyant gas prior to cruise, with a large reduction in frontal area, and thus a more efficient cruise flight configuration.

Drag coefficient should be less and lift-drag ratios greater for parawing configurations. However, two factors work simultaneously to complicate the picture and reverse the advantage in flight efficiency to favor the Dynastat configuration. First, the parawing must aerodynamically lift all of the vehicle weight, while the Dynastat aerodynamically lifts the total weight decreased by the net buoyant lift. Therefore, if half the vehicle lift is supplied by buoyancy, in order for the parawing to be competitive it would require twice as high an aerodynamic lift-drag ratio. Secondly, both vehicles operate at lift coefficients so far below that required for maximum lift-drag ratio, that the cruise lift-drag ratio is more strongly a function of cruise conditions rather than ideal efficiency of the configuration. When a buoyant system is designed to lift an appreciable portion of the vehicle weight for vertical takeoff at low power, the system is so large that at reasonable altitudes it must operate at very low lift coefficients. The effect of operating the two configurations at low lift coefficients is seen in figure 9, which shows drag coefficient and lift-drag ratio as a function of lift coefficient. While the maximum lift-drag ratio of the parawing is almost 40% greater, the operating lift-drag ratio becomes less than Dynastat, and drag coefficient becomes greater, at lift coefficients below 0.4. The operating region of the two configurations sized for VTOL is presented in figure 10, which shows percent of propulsive lift, and maximum lift-drag ratios as functions of lift coefficient. It is apparent that for almost all of the propulsive range studied, both configurations are operating at such low lift coefficients, that the most efficient configuration is established by operating conditions rather than maximum configuration efficiency.

From a performance standpoint, the data indicates that the Dynastat configuration has a distinct advantage over parawings in the VTOL mode of operation. A Dynastat vehicle with buoyancy providing 20% to 80% of the takeoff lift, would have cruise velocities between 100 and 250 mph (161 and 403 km/hr) and cruise ranges from 200-400 miles (322-644 km). This broad range of design parameters might be sufficient to permit an optimum design between cost, which increases with propulsive lift, and operational problems, which increase with buoyant volume.

Results of the VTOL study indicated that some advantage might be realized if the configurations were designed as STOL vehicles. In requiring sufficient lift for VTOL, either the buoyancy system must be so large that inefficient cruise lift coefficients result, or required power is so high that the attractiveness of such systems over non-buoyant VTOL configurations is greatly diminished.

Short Takeoff and Landing

Dynastat.- While the primary intent was to examine sizing relationships conducive to short landing strip lengths, the decision was made to restrict cruise operation to lift-drag ratios of at least 80% of the maximum lift-drag ratio. For the Dynastat configuration, figure 10 indicates that this condition will prevail for lift coefficients between .12 and .515. Therefore, all Dynastat data was obtained at these two lift coefficients in addition to the lift coefficient for maximum lift-drag ratio, .26. Such limits are artificial, but are probably practical from a design standpoint, and provide a convenient constraint on the analysis.

The variation of cruise altitude with cruise velocity is presented in figure 11 for buoyant volumes ranging from 25,000 ft^3 to 150,000 ft^3 (708 m^3 to 4246 m^3). Cruise altitudes of 5000 to 10,000 ft (1524 to 3048 m) were considered in subsequent examination of the data.

The data in figure 11 were used to determine the minimum and maximum cruise velocities for the STOL Dynastat configuration. It is apparent aerodynamically that the minimum cruise speed will occur at the maximum lift coefficient and minimum altitude within the stated constraints, and the maximum cruise speed will occur at minimum lift coefficient and maximum altitude. Such speed limits were obtained by cross-plotting the figure 11 data, and are presented in figure 12, which shows the relationship between buoyant volume and cruise velocity. The area between the outermost curves represents the available design region. Also shown in figure 12 is the relationship between buoyant volume and cruise velocity for operation at maximum lift-drag ratio.

The next significant parameter examined was required horsepower. Figure 13 presents the variation of rated sea-level shaft horsepower as a function of cruise velocity. The lower flat portion of the curves comprises the region where power requirements are established by the condition that thrust be 25% greater than drag at take-off. At higher velocities, power is established by the condition that thrust equals drag at cruise. The data in figure 13 were cross-plotted to show the influence of buoyant volume on cruise velocity for assumed constraints on power, and are presented in figure 14. The dashed curves in figure 14 are the curves presented previously in figure 12. The 50% and 100% power curves are

referenced to power required for the tilt rotor VTOL referred to earlier from reference 3. The minimum power curve was generated from the maximum velocity points on the flat portion of the curves in figure 13. Since a primary reason for considering buoyant systems is to minimize power requirements, thereby alleviating pollution, noise, and cost characteristics, the minimum power curves in figure 14 will be established as a design constraint in the current evaluation. The vehicle will be considered to be power limited, and the maximum cruise velocity at a given lift coefficient is represented by the minimum power curves in figure 14.

It is apparent from figure 14(a) that the previously established aerodynamic velocity limits at 5000 and 10,000 ft (1524 and 3048 m) altitude are not valid limits since insufficient power is available. A more valid maximum speed curve is that shown in figure 14(b) for flight at maximum lift-drag ratio at an altitude of 5000 ft (1524 m). Sufficient power is available for flight at these conditions, with buoyant volumes between 37,000 ft^3 and 110,000 ft^3 (1047 m^3 and 3114 m^3). For sea level flight at C_L = .515, sufficient power is available for all buoyant volumes less than 145,000 ft^3 (4104 m^3). Therefore the previously obtained minimum velocity curve is valid for these buoyant volumes. The available design region previously shown in figure 12, has been redrawn with the power constraints, and is presented in figure 15.

Landing field length is presented in figure 16 as a function of cruise velocity. Three vehicle lengths have been added to the takeoff length to obtain values of field length which are consistent with those for the semi-buoyant VTOL vehicles in the first phase of the study. The decrease in field length at higher cruise velocities results from higher takeoff

accelerations due to the higher engine powers required for these flight speeds. Since the higher powers have already been rejected previously with the imposed power constraint, only the flat portions of these curves will be considered. The field lengths are shown as a function of buoyant volume in figure 17. The curve is identical for all three values of cruise lift coefficient. By establishing the constraint that only field lengths within 10% of the minimum length shown will be allowed, a lower limit of 55,000 ft^3 (1557 m^3) is obtained for buoyant volume. This is a rather arbitrary constraint, but its influence is relatively small. Its only influence is on cruise velocity, and by eliminating the constraint, velocity could only be increased 31 mph (50 km/hr) before running into the previously established power constraint. Figure 18 presents the newly established design region with the field length constraint.

Within the design region of figure 18, vehicle range shows little change with either speed or buoyant volume. At a C_L of .26, range equals approximately 400 miles (644 km), and at C_L = .515 it equals about 300 miles (483 km). This is consistent with the difference in lift-drag ratio at these values of C_L.

Having established a design region and a number of the more pertinent vehicle characteristics for an STOL semi-buoyant system, it is beneficial to compare such a vehicle with the semi-buoyant VTOL systems examined in the first phase of this study. For cruise velocities of 100-200 mph (161-322 km/hr), the VTOL system required propulsive lifts from 14% to 60%. A comparison of the vehicles designed for the two modes of operation is presented in the following table.

	VTOL	STOL
Buoyant Volume-ft^3 (m^3)	350,000-750,000 (9,915-21,230)	55,000-145,000 (1,557-4,106)
Vehicle Length-ft (m)	215-270 (65.5-82.3)	115-155 (35.0-47.2)
Field Length-ft (m)	645-810 (196.6-246.8)	720-790 (219.5-240.8)
Required Horsepower	1500-6000	4200-4900
Range - miles (km)	250-475 (402-764)	300-400 (482-644)

Except for vehicle size, there appears to be little difference between the two vehicles. However, a characteristic which has not been previously discussed, provides a basis for choice. For the VTOL vehicle, takeoff and landing accelerations are negligible, but for the STOL vehicle, they vary between 0.4 and 0.5 g's, because the low lifting capacity of these vehicles requires a high takeoff velocity. This is excessive for commercial passenger operation. They could of course be cut in half merely by throttling the engines on takeoff, but field length would be doubled making the vehicle less competitive.

Parawing.- As in the case of the helium vehicle, data was obtained at maximum lift-drag ratio, and 80% of maximum lift-drag ratio. Cruise conditions corresponding to this constraint were: C_L = .545, L/D = 7.52; C_L = 1.14, L/D = 9.40; and C_L = 2.17, L/D = 7.52. Data corresponding to that for the helium vehicle in figures 11-18, is presented for the hot-air vehicle in figures 19-25. These data indicate, figure 25, a design region with cruise velocities between 80 mph and 145 mph (129 km/hr and 233 km/hr), for buoyant volumes from 23,000 ft^3 to 30,000 ft^3 (651 m^3 to 849 m^3). Volume can be extended beyond the upper limit, but the lower resulting cruise velocities would probably be less desirable. Within the minimum power constraint, the hot-air vehicle had a takeoff acceleration of only .25 g's, which is marginal for commercial passenger transportation.

Performance and sizing characteristics for the hot-air STOL vehicle with a cruise velocity of 136 mph (219 km/hr) and a buoyant volume of 23,000 ft^3 (651 m^3) are compared to the other VTOL and STOL vehicles examined in this study in table II. The parawing STOL vehicle is superior to the Dynastat STOL vehicle in every respect except field length, and the difference there is insufficient to consider the Dynastat vehicle competitive. The parawing STOL vehicle is superior to the VTOL vehicles in every respect except field length and acceleration. Since its advantage in size, power requirements, and range is so great, it seems probable that some of the constraints on the parawing STOL vehicle could be modified to reduce acceleration to a lower level and still have a vehicle distinctly superior to the VTOL configurations.

CONCLUDING REMARKS

Four configurations have been studied in this investigation; Dynastat VTOL and STOL, and parawing VTOL and STOL. Of the four, the parawing VTOL and the Dynastat STOL do not appear sufficiently competitive with the others to warrant continued study. The parawing VTOL requires the shortest field length, but none of the vehicles required more than about an 800 foot field which should be sufficiently short for most purposes. On the negative side, the parawing VTOL was much larger than the STOL vehicles, and exhibited considerably shorter range than any of the other vehicles. The Dynastat STOL is considerably larger than the parawing STOL, requires considerably more power than either that vehicle or the Dynastat VTOL, and had an excessive takeoff acceleration for a commercial passenger transport. While the latter

factor is subject to change through modified design procedures, such changes would result in the further deterioration of other performance characteristics.

At cruising speeds between 125 and 150 mph (201 and 241 km/hr), the parawing STOL configuration appears to have an advantage over the Dynastat VTOL configuration. It is only 30% as long, requires 30% less power, and has 50% greater range, while requiring about the same field length. However, for cruise speeds up to 125 mph (201 km/hr), the Dynastat VTOL configuration is superior in both power requirement and range, and remains inferior only in size. For speeds above 150 mph (241 km/hr), it is uncertain from the present data which configuration is superior. If the constraints establishing the design region in Figure 25 are retained, then the hot-air STOL vehicle cannot be designed for speeds greater than 150 mph (241 km/hr). However, these constraints need not be rigid, and easing of the field length and minimum power restrictions, could permit cruise speeds of more than 300 mph (482 km/hr), with required power still remaining below that for the Dynastat VTOL configuration.

Comparison of these vehicles with the tilt-rotor VTOL of NASA CR-902 indicates that they require about one-fourth the power at cruise speeds below 150 mph (241 km/hr), and have a distinctly greater range at these speeds. The data shows a continued, though decreasing superiority over the tilt-rotor vehicle throughout the speed range studied, but there is a serious question as to how high a speed flexible and buoyant systems can operate before the design problem becomes significantly more difficult. The Dynastat proposal called for a maximum speed of 138 mph (222 km/hr) at 3000 ft (915 m) altitude. This corresponds to a speed of 153 mph (246 km/hr) at 10,000 ft (3048 m) altitude, to give the same dynamic pressure of 44.5 lbs/ft^2 (213 N/m^2). Higher limits to velocity and dynamic pressure remain to be determined in a more complete study.

The study has indicated that there may be a distinct advantage for buoyant and flexible systems in the cruise speed range below 150 mph (241 km/hr). However, a firm conclusion of that nature would require point design studies considerably greater in depth. Such studies would first establish a reasonable upper limit on cruise velocity for the operation of flexible vehicles. Then detailed engineering calculations would be performed for both Dynastat and parawing vehicles at this cruise speed, at 150 mph (241 km/hr), and probably at some lower velocity. Field length limitations of both 1000 and 2000 ft (305 and 610 m) should be considered, and a more rational estimation should be obtained for the various quantities which had to be assumed in this study. Finally, an economic comparison of such systems with other proposed short-haul flight systems and ground systems should be made.

REFERENCES

1. Proposal for 35 Passenger "Dynastat" Transporter, Goodyear Aerospace Corporation, June 30, 1969, GAP-5501.

2. Polhamus, Edward C.; and Naeseth, Rodger L.: "Experimental and Theoretical Studies of the Effects of Camber and Twist on the Aerodynamic Characteristics of Parawings Having Nominal Aspect Ratios of 3 and 6," NASA TN D-972, 1963.

3. "Study of the Feasibility of V/STOL Concepts for Short-Haul Transport Aircraft," Lockheed-California, NASA CR-902, October 1967.

4. "Prop-Fan," Hamilton-Standard, July 1, 1970.

5. Hoerner, Dr. -Ing S. F.: "Fluid-Dynamic Drag," published by the author, 1965.

6. Havill, Lt. Clinton H., U.S.N.: "The Drag of Airships," NACA TN-247, September 1926.

7. Durand, W. F.: "Aerodynamic Theory, Vol. VI," published by Berlin Julius Springer, 1936.

APPENDIX A

AERODYNAMICS ESTIMATION FOR DIRIGIBLES

An estimate was made of the lift and drag characteristics of the Dynastat configuration proposed by the Goodyear Aerospace Corporation (figure 1). The procedure used to estimate the zero-lift drag will be described first, followed by the methods used for the lift and induced drag.

Zero-Lift Drag

The zero-lift drag was estimated by summing the individual component drag coefficients, as shown in the following equation:

$$C_{D_{\Delta_o}} = C_{D_{\Delta_{BAG}}} + C_{D_{\Delta_{FINS}}} + C_{D_{\Delta_{NACELLES}}} + C_{D_{\Delta_{STRUTS}}}$$

where C_{D_Δ} represents the drag coefficient based on the reference area S_Δ equal to bag volume, V. to the 2/3 power. $S_\Delta = (800{,}000)^{2/3} = 8600$ sq. ft. for the Dynastat. The component drags were estimated as follows:

Bag Drag

The equation used for the $C_{D_{\Delta_{BAG}}}$ was obtained from ref. 5, pg. 6-19, equation 36.

$$C_{D_{\Delta_{BAG}}} = c_f \left[4\,(l/d)^{1/3} + 6\,(d/l)^{1/2} + 24\,(d/l)^{2.7}\right]$$

where l/d = effective fineness ratio. The l/d for the non-circular Dynastat configuration was calculated by estimating the maximum cross-sectional area ($A_{TT_{MAX}}$), determining the equivalent circular cross-section diameter with the same area, and dividing this into the body length. For the Dynastat,

$$A_{TT_{MAX}} = 5006 \text{ sq. ft. and, } l/d = \frac{292}{2\sqrt{\frac{A_{TT_{MAX}}}{\pi}}} = 3.67$$

For V = 105 knots at sea level, the Reynolds number is 3.29×10^8 for a reference length of 292 ft. At this Reynolds number the skin friction coefficient c_f is approximately .0016. Therefore, $C_{D_{\Delta_{BAG}}} = .0138$. At slower speeds, the Reynolds number is smaller and the c_f is larger; for example, at V = 45 knots, Re = 1.41×10^8, $c_f = .002$, and $C_{D_{\Delta_{BAG}}} = .0172$.

Fin Drag.- Assuming a fin thickness ratio of 10% and a c_f of .0025, the fin drag coefficient may be estimated from ref. 5, pg. 6-9, figure 10. $C_{D_{FINS}}$ based on frontal area = .06. The total frontal area for the three fins for the Dynastat is approximately 570 sq. ft. Basing the fin drag coefficient on the Dynastat S_Δ gives the fin drag component as:

$$C_{D_{\Delta_{FINS}}} = .00398$$

Nacelle Drag.- From ref. 5, pg. 9-9, Figure 12, the nacelle drag for turbulent flow based on nacelle frontal area is:

$$C_{D_{NACELLES}} = .055$$

The frontal area of the 6 nacelles on the Dynastat is approximately 64.4 sq. ft. This nacelle drag coefficient based on the Dynastat S_Δ is:

$$C_{D_{\Delta_{NACELLES}}} = .00041$$

Strut Drag.- Assuming a strut thickness ratio of 10% and c_f of .0025, the strut drag coefficient may be estimated from ref. 5, pg. 6-9, figure 10. $C_{D_{STRUTS}} = .06$ based on frontal area. The total frontal area of the 6

nacelle struts on the Dynastat is approximately 118.8 sq. ft. Basing the nacelle drag coefficient on the Dynastat S_Δ gives:

$$C_{D_{\Delta_{STRUTS}}} = .00083$$

Adding the foregoing drag components, the total zero-lift drag coefficient of the Dynastat is approximately:

$$C_{D_{\Delta_o}} = .0138 + .00398 + .00041 + .00083$$

$$C_{D_{\Delta_o}} = .0190 \text{ @ } V = 105 \text{ knots}$$

or, $$C_{D_{\Delta_o}} = .0224 \text{ @ } V = 45 \text{ knots}$$

It is interesting to note that the value of zero lift drag coefficient obtained by this procedure, .019, is very close to the value presented in reference 6 for a well-designed dirigible.

Lift

The lifting characteristics for the Dynastat were estimated using equations for small aspect ratio (AR) wings given in ref. 5, pg. 7-16, eqn. 30 & 31. Combining the first and second components of lift given by these equations gives:

$$C_L = 0.5 \pi AR \sin \alpha + k \sin^2 \alpha \cos \alpha$$

based on wing planform area.

The AR of the Dynastat was estimated as

$$AR = \frac{\text{span}^2}{\text{plan area}} = \frac{(120)^2}{27090} = 0.531,$$

and k = 1.5 for AR = 0.531, from ref. 5, pg. 7-18, figure 30.

The lift coefficient, based on the Dynastat S_Δ, becomes:

$$C_{L_\Delta} = 2.72 \sin \alpha + 4.90 \sin^2 \alpha \cos\alpha$$

Induced Drag

The induced drag component (drag due to lift) can be estimated approximately as the product of lift and tan α (ref. 7, pg. 96-97). This holds true for dirigible hulls, with or without fins and struts attached, within a wide range of angles of attack, α. Therefore:

$$C_{D_{INDUCED}} = C_{L_\Delta} \tan \alpha$$

B-1

APPENDIX B

PARAWING SIZING

A double-layered parawing was assumed, with the space between the two layers inflated during the buoyant lift phase as indicated in figure 1(b). The parawing chosen was the cylindrical model in reference 2, with an aspect ratio of 2.7. Its flat planform dimensions are shown in figure 26. The upper sketch shows the actual model dimensions tested in the reference 2 study, while the lower sketch shows the geometric representation of one side of the model, which was used to develop the relationship between planform area and volume presented below. This was done to convert the aerodynamic coefficients in reference 2 to a volume base, which was more convenient for the present analysis.

It was assumed that each side of the parawing would inflate to produce a conical volume capped by a hemisphere at its trailing edge.

The juncture of the cone and sphere will occur in a flat planform representation at a distance forward of the base equal to 1/2 the width of the cone triangle at that point (see geometric sketch in figure 26). The total height of the flat planform cone is

$$h_t = 51.37 \cos (20.885°) = 47.97 \text{ ft}$$

At the cone sphere juncture, the ratio of 1/2 the width to the cone length forward of that point is given by

$$\frac{x}{h_c} = \tan (20.885°) = .3815$$

also

$$x = h_t - h_c = 47.97 \text{ ft} - hc$$

and combining these equations gives x = 13.25 ft. In the inflated condition, the cone base perimeter, equal to the hemisphere perimeter, is equal to 4x, or the corresponding radii are

$$r_c = \frac{4x}{2} = 8.44 \text{ ft} = .7035 \text{ ft}$$

and

$$h_c = \frac{13.25}{.3815} = 34.73 \text{ ft} = 2.894 \text{ ft}$$

The volume of the cone is $v_c = 1.047\ (.7035)^2\ (2.894) = 1.5\ ft^3$. The volume of the hemisphere is $v_s = 4.189\ (.7035)^3 = 1.459^3$.

The volume of one wing is 2.959 ft^3 and the total volume is twice this, or

$$V_B = 5.918\ ft^3$$

The aerodynamic data in reference 2 are based on a flat planform area of 11.88 ft^2. This corresponds to

$$(V_B)^{2/3} = (5.918)^{2/3} = 3.274\ ft^2$$

and the conversion factor in making the transformation is

$$\frac{11.88}{3.274} = 3.627$$

TABLE I. PROPULSION SYSTEM CHARACTERISTICS

PARAMETER	PROPS	PROP-FANS	FANS
(F_o/P_o)	4.5	2.5	1.2
a	.27	.53	1.02
$b \times 10^6$	2.992	2.453	2.082
K_E	.18	.21	.255

TABLE II. CONFIGURATION CHARACTERISTICS

Cruise Velocity = 136 mph (219 km/hr)

PARAMETER	VTOL		STOL	
	DYNASTAT	PARAWING	PARAWING	DYNASTAT
BUOYANT VOLUME - ft^3 (m^3)	600,000 (16,990)	460,000 (13,040)	23,000 (652)	127,000 (3,595)
VEHICLE LENGTH - ft (m)	263 (80.2)	185 (56.4)	80 (24.4)	145 (44.2)
FIELD LENGTH - ft (m)	789 (240.6)	555 (169.2)	802 (244.5)	657 (200.2)
REQUIRED HORSEPOWER	3100	7200	2200	4400
RANGE - miles (km)	340 (547)	141 (243)	508 (817)	350 (563)
TAKEOFF ACCELERATION - g's	---	---	.25	.45

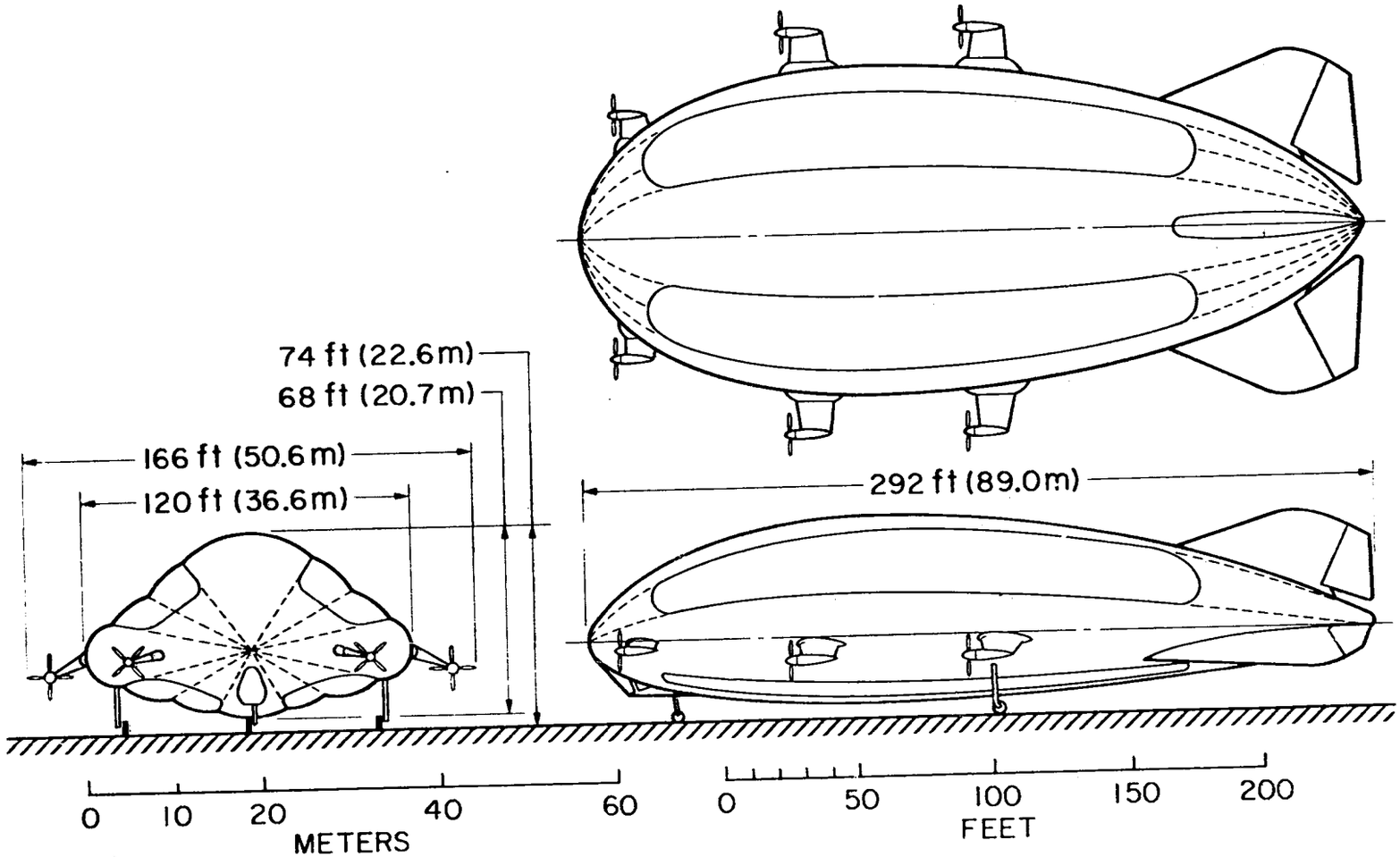

Figure 1.- Study Configurations.

(a) Dynastat

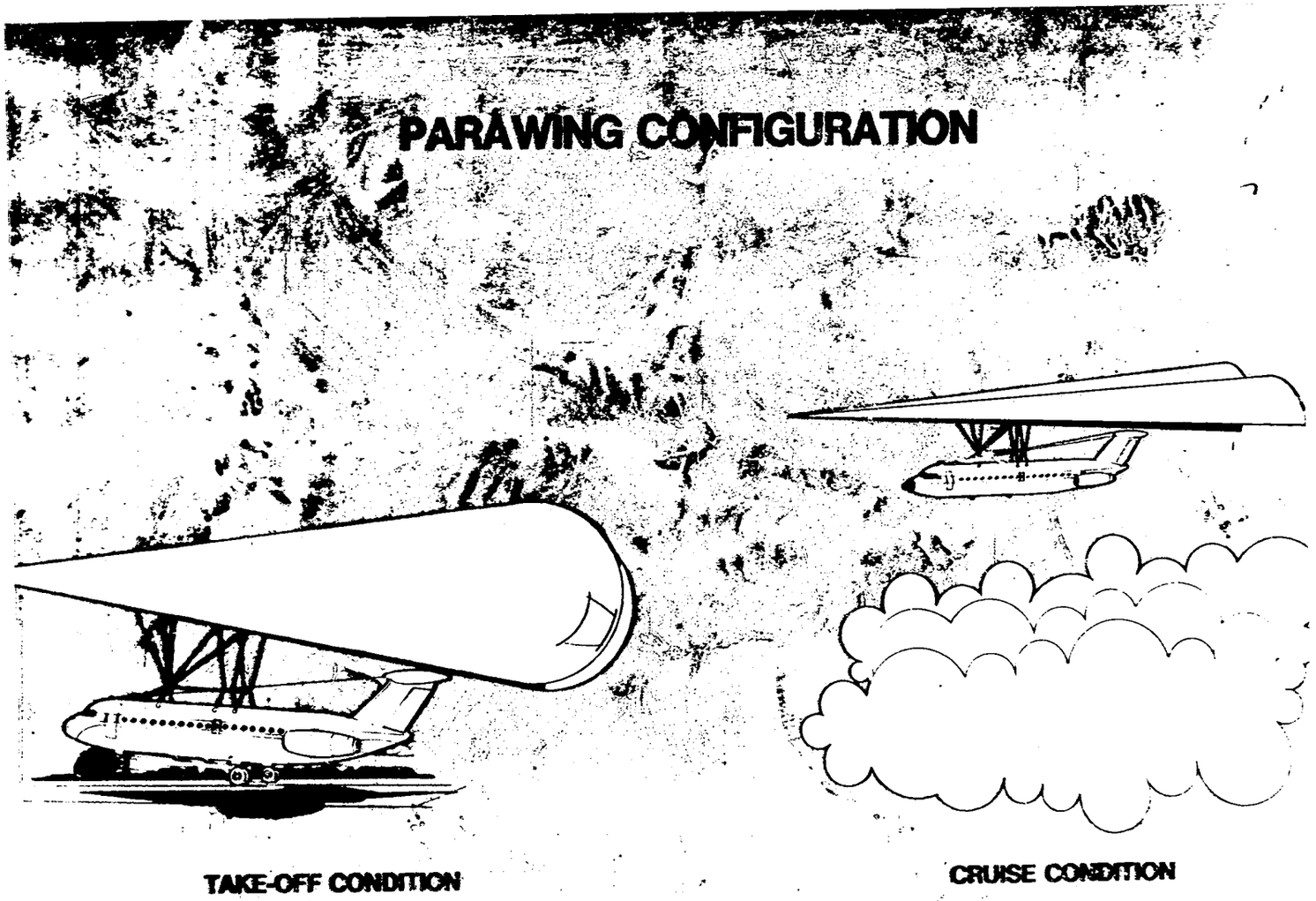

Figure 1.- (Concluded)
(b) Parawing

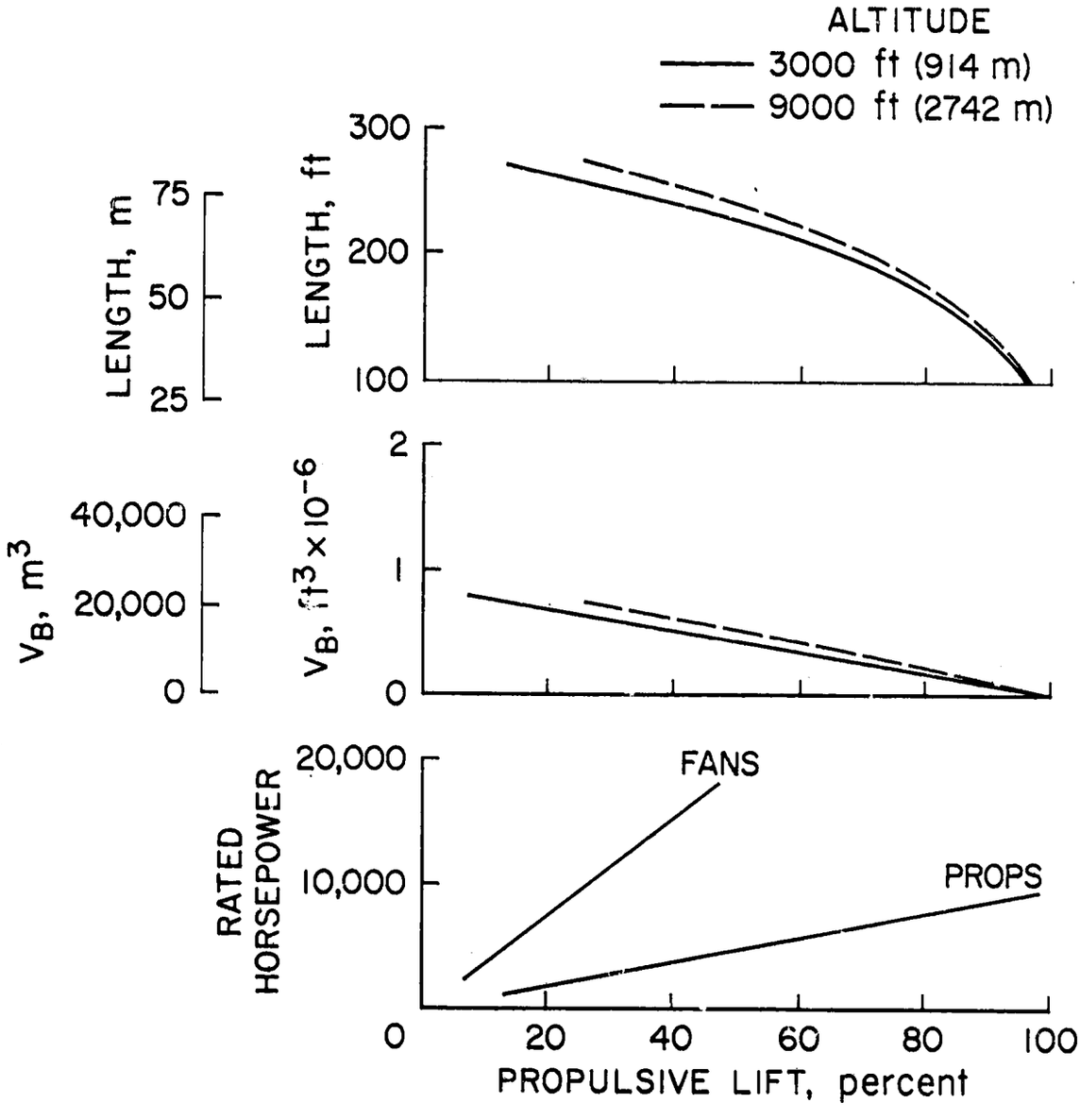

Figure 2.- Dynastat Sizing Parameters.

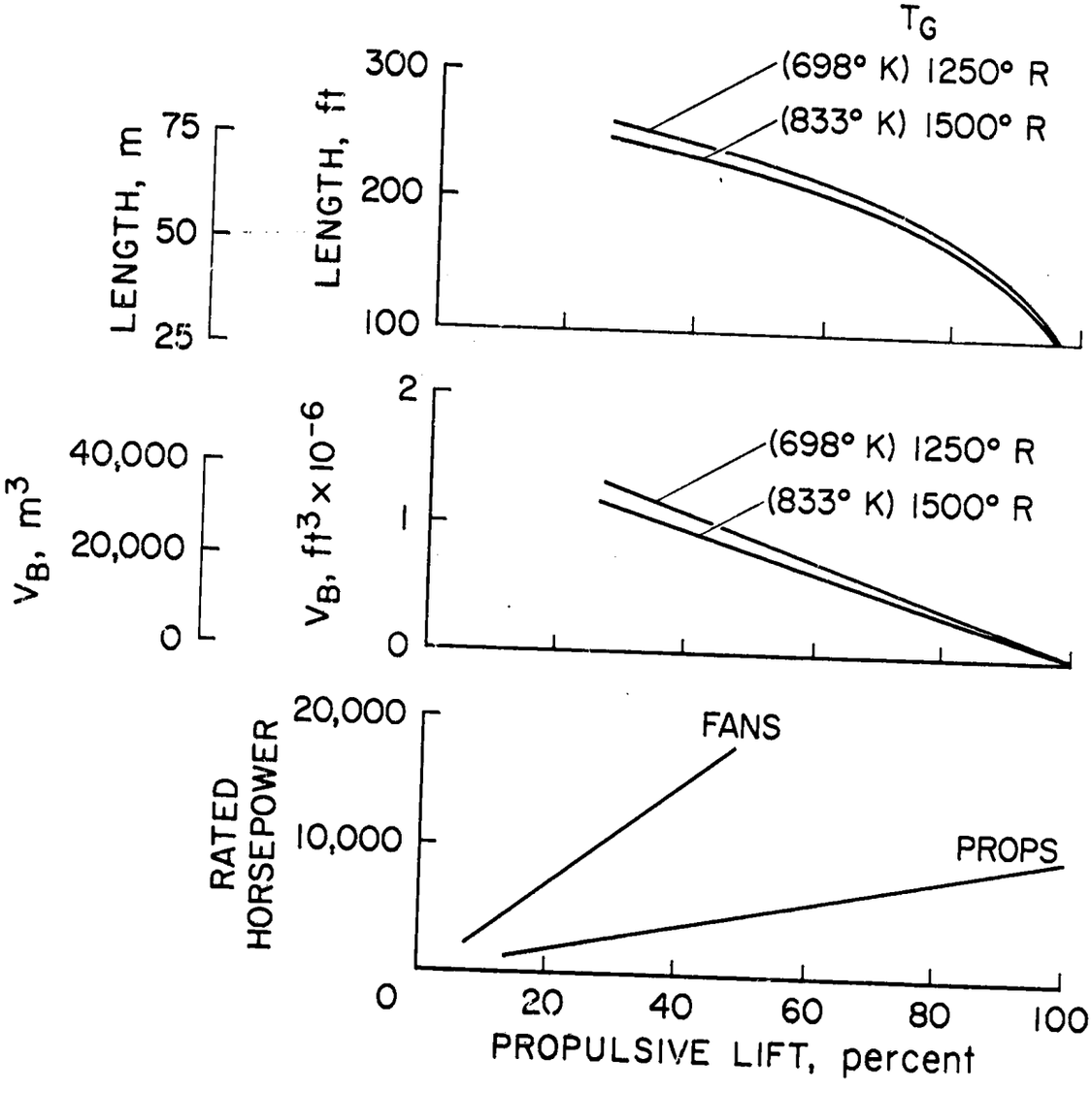

Figure 3.- Parawing Sizing Parameters.

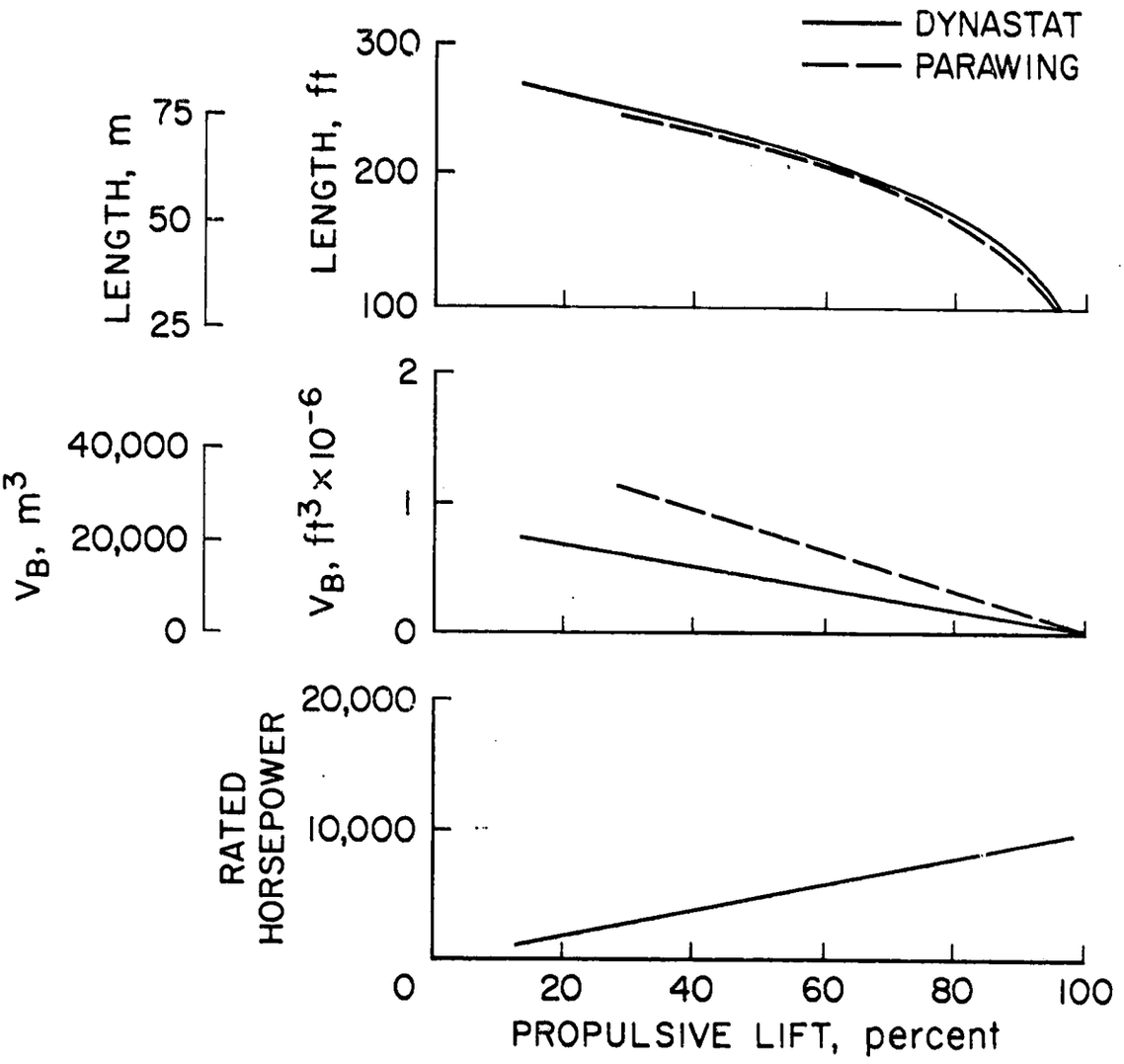

Figure 4.- Comparison of Dynastat and Parawing Sizing Parameters.

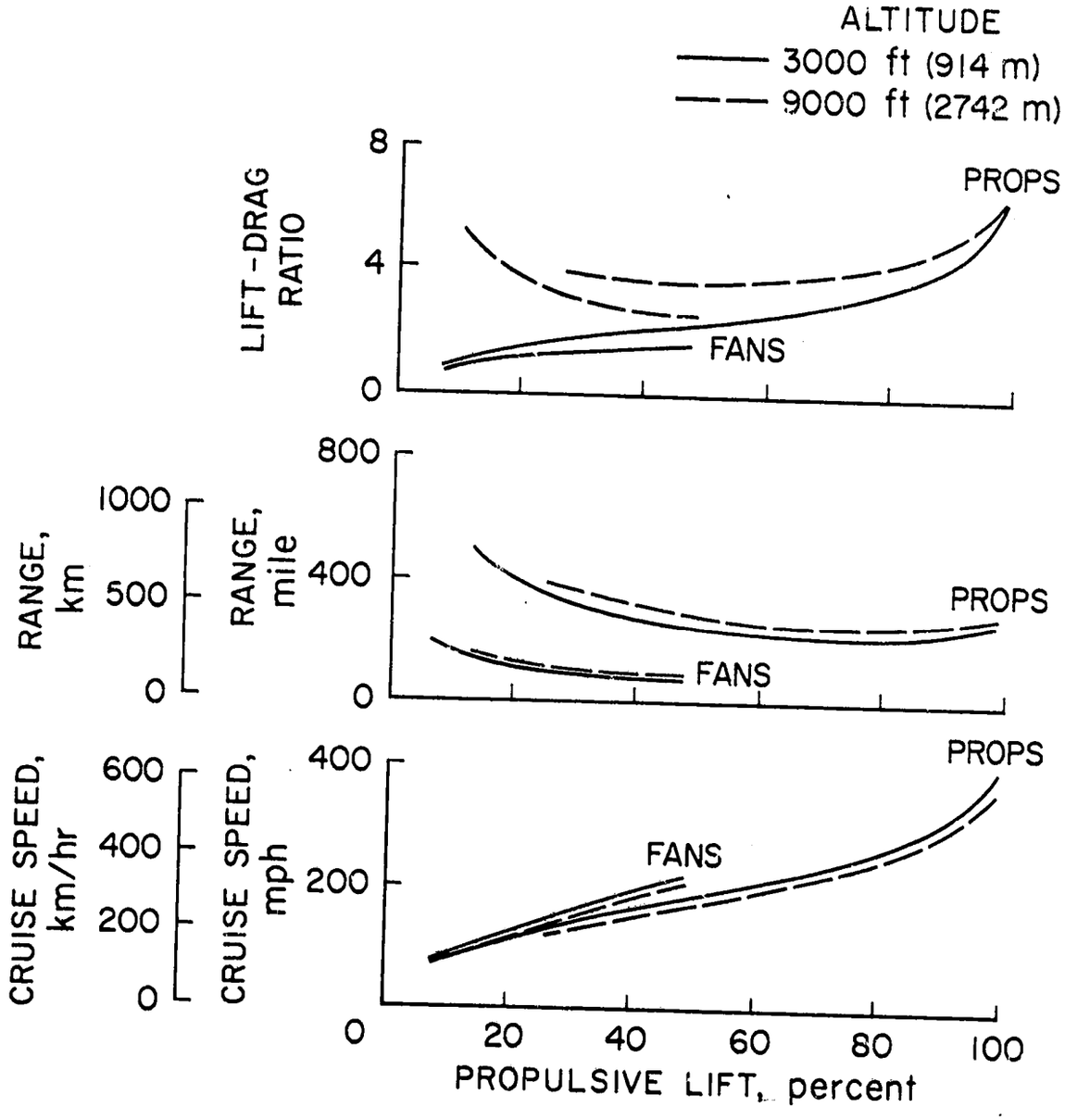

Figure 5.- Dynastat Performance Parameters.

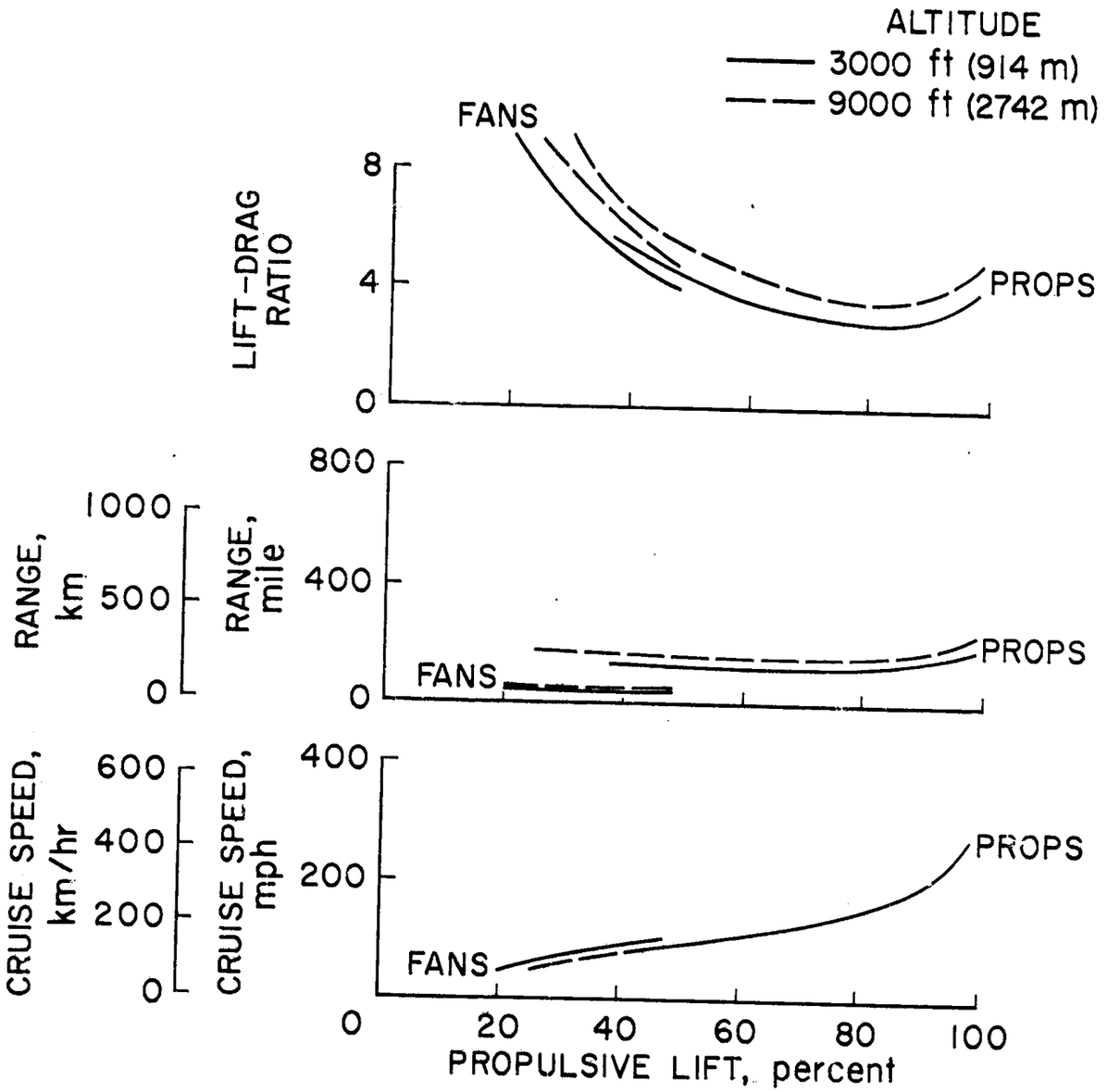

Figure 6.- Parawing Performance at T_G = 1250°R.

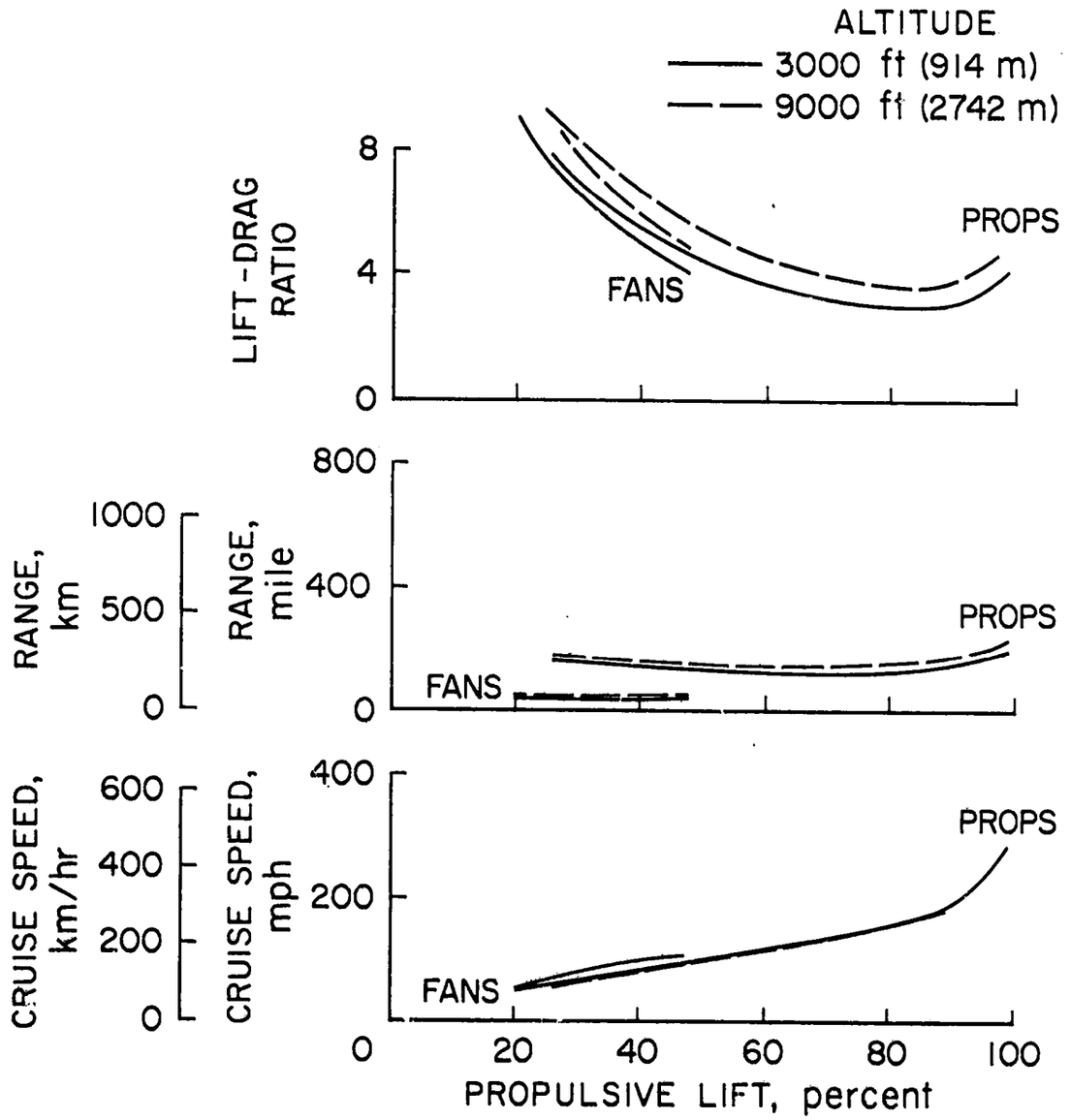

Figure 7.- Parawing Performance at T_G = 1500°R.

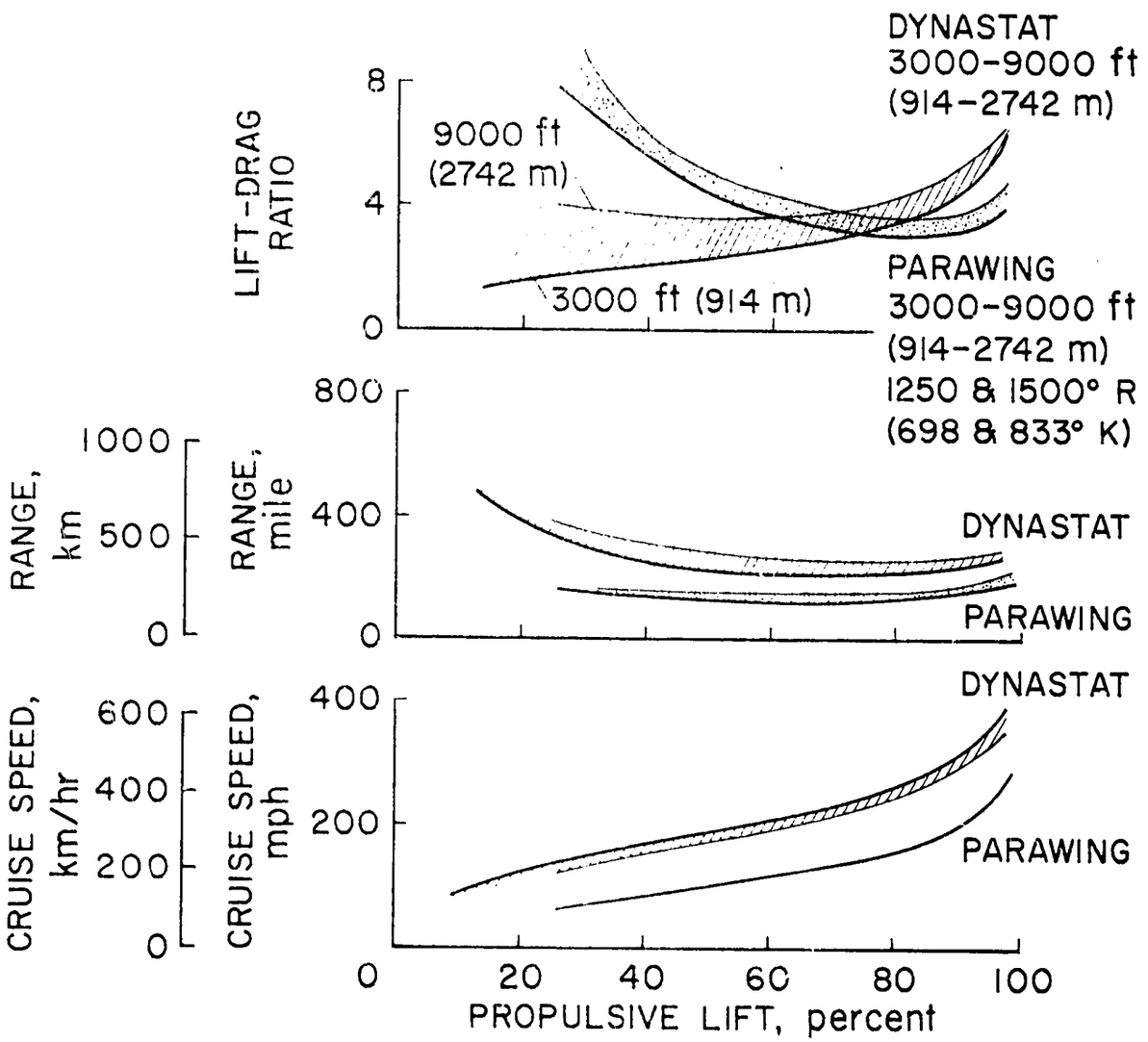

Figure 8.- Comparison of Dynastat and Parawing.

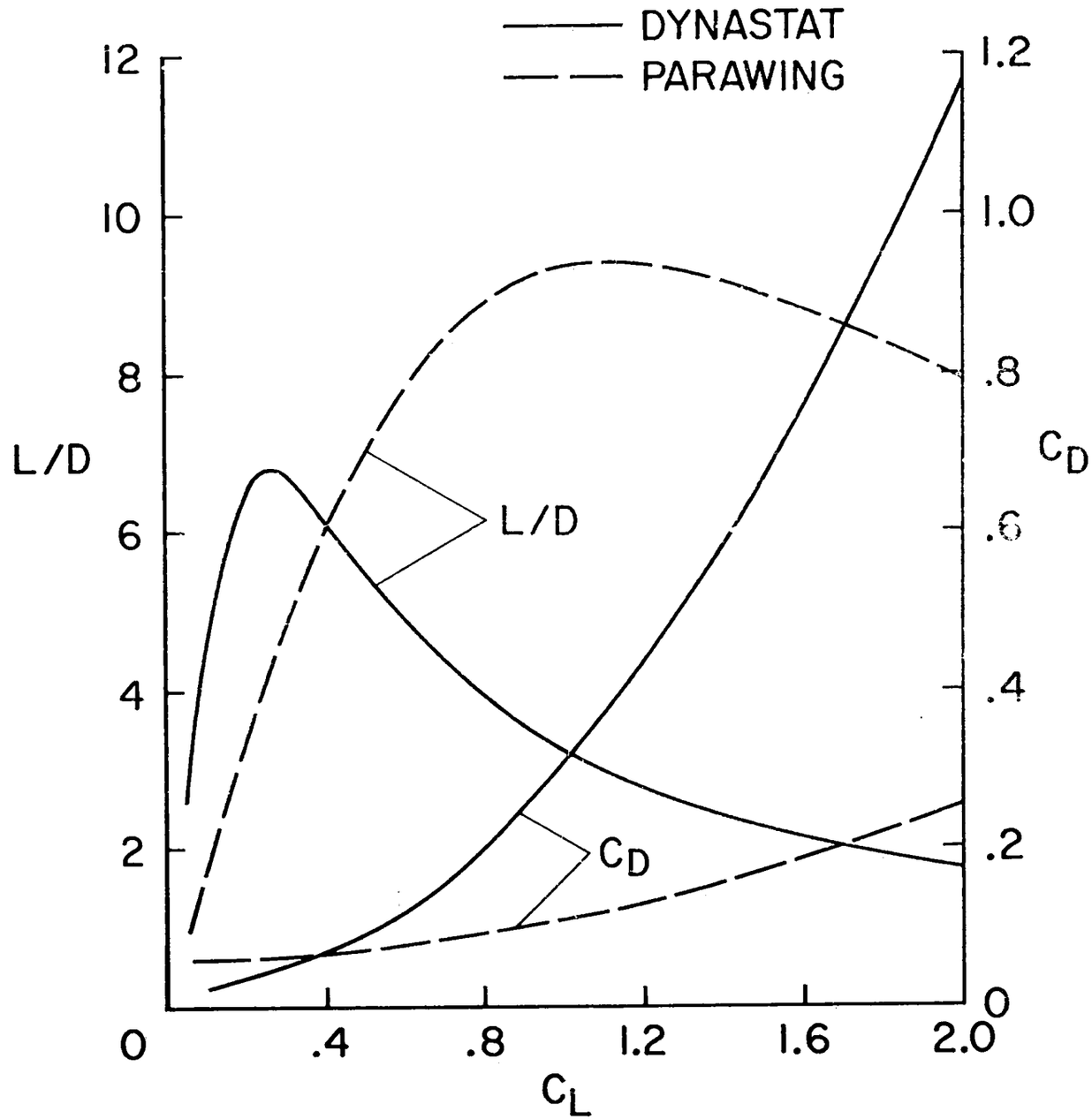

Figure 9.- Configuration Aerodynamics.

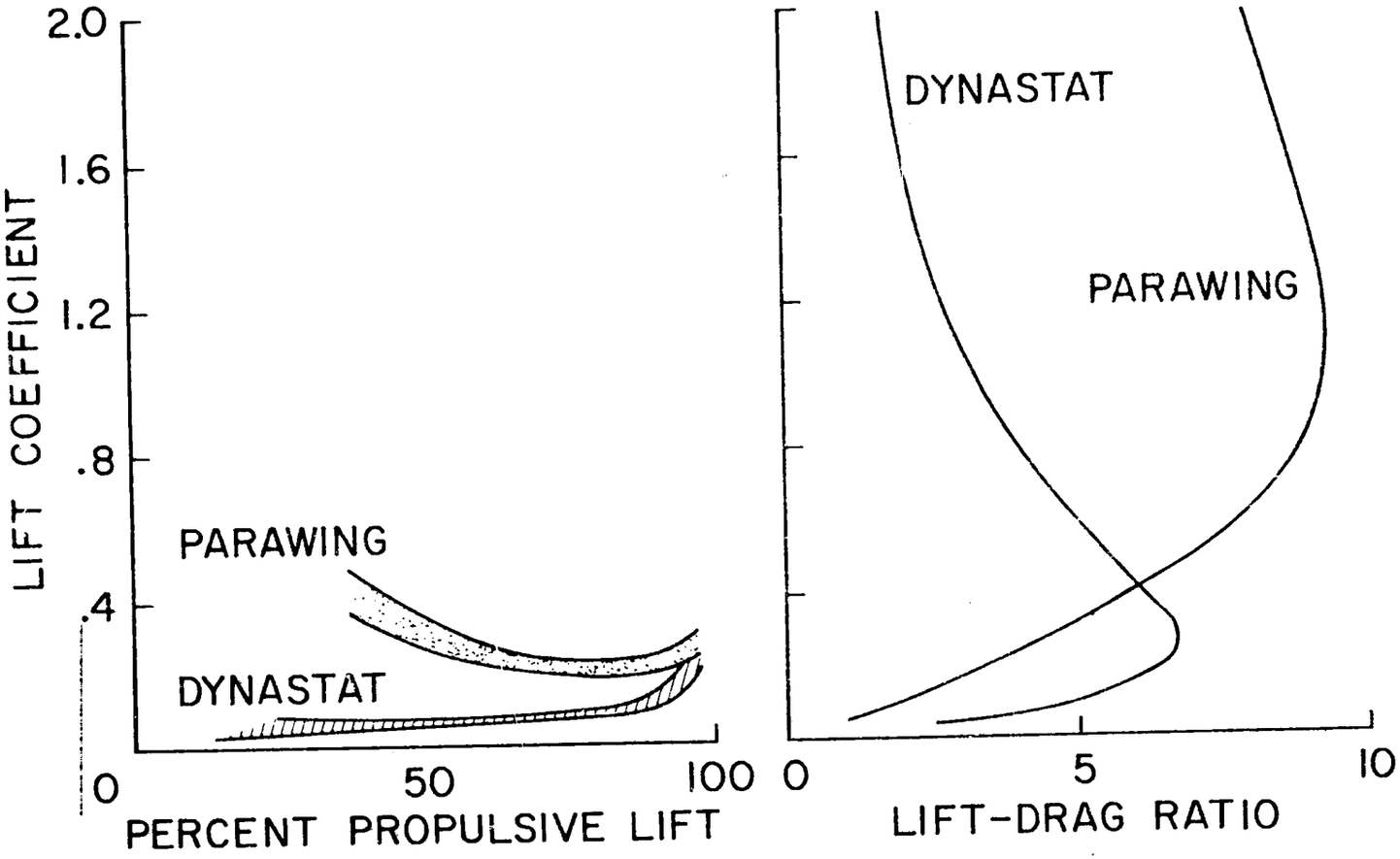

Figure 10.- Aerodynamics and Propulsive Lift.

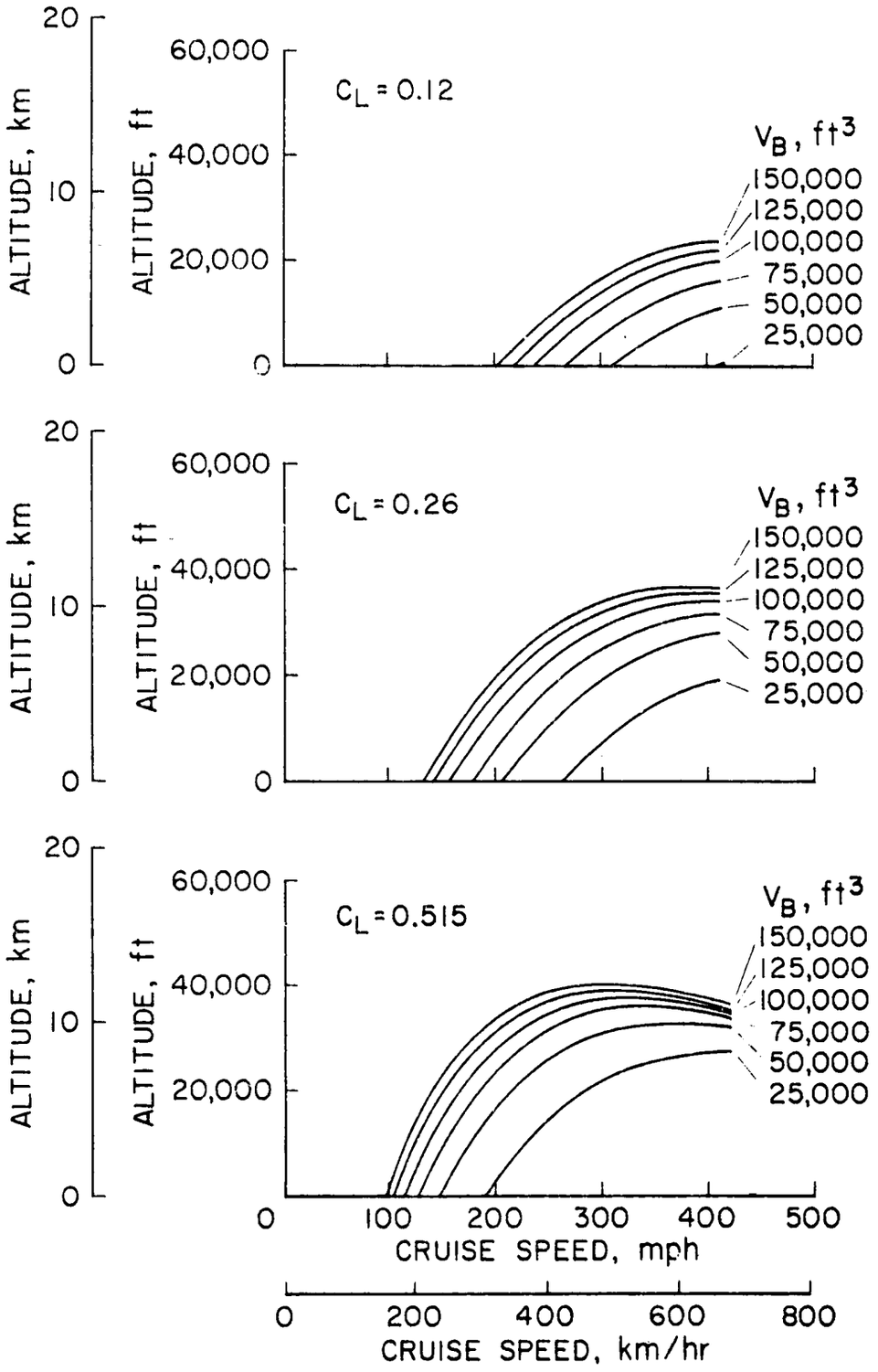

Figure 11.- Dynastat Equilibrium Altitude.

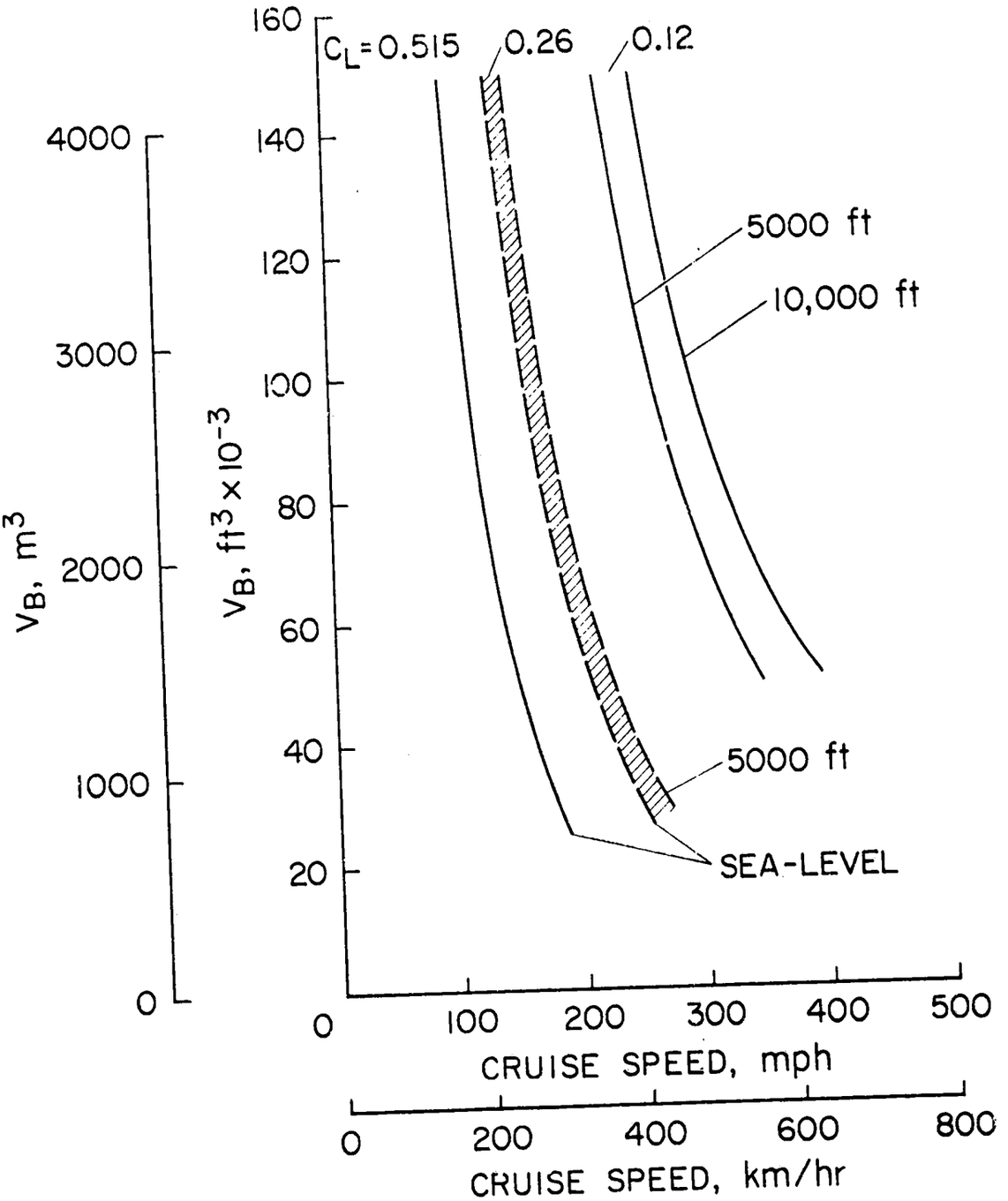

Figure 12.- Dynastat Equilibrium Buoyancy

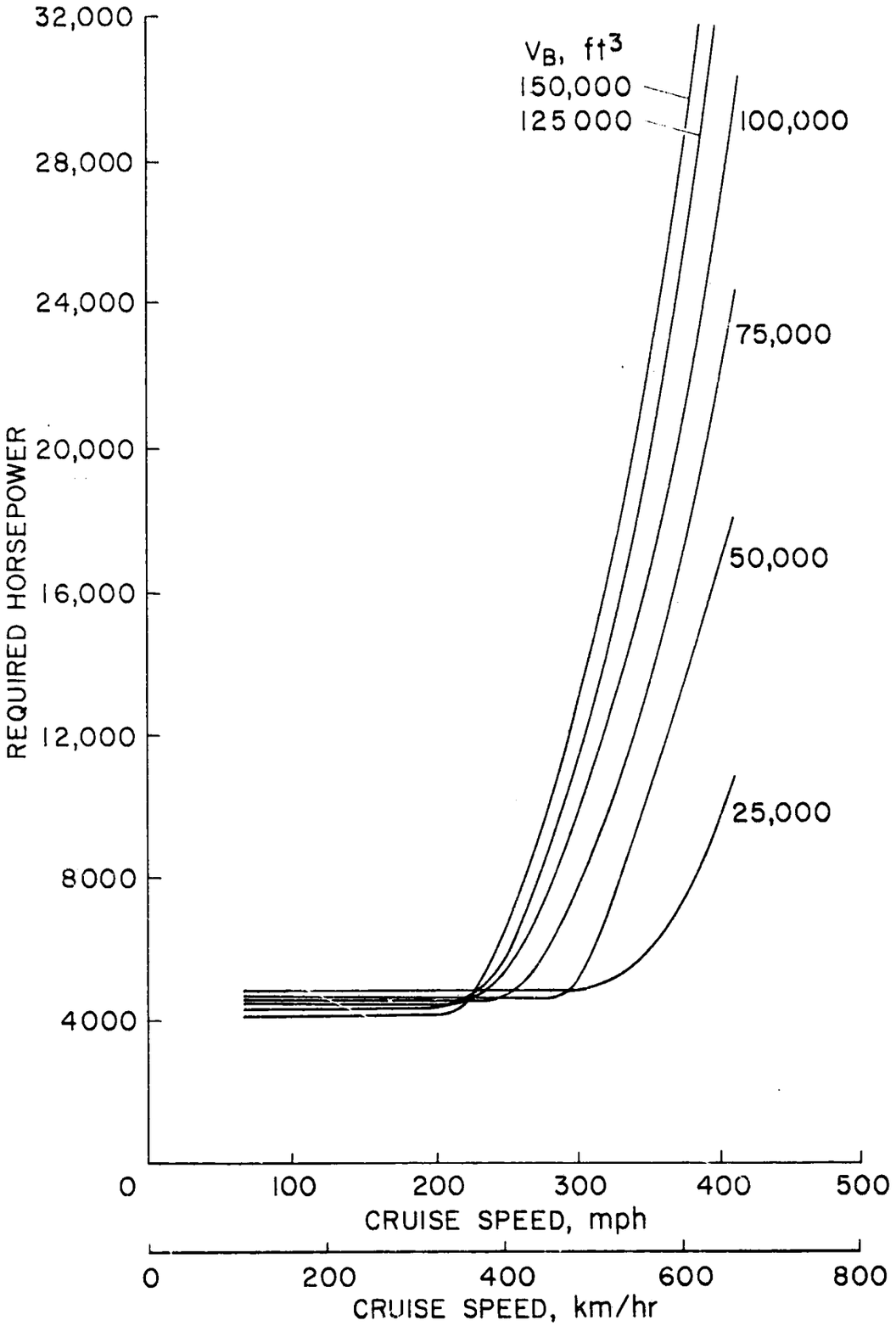

Figure 13.- Dynastat Horsepower Requirements.
(a) C_L = .12

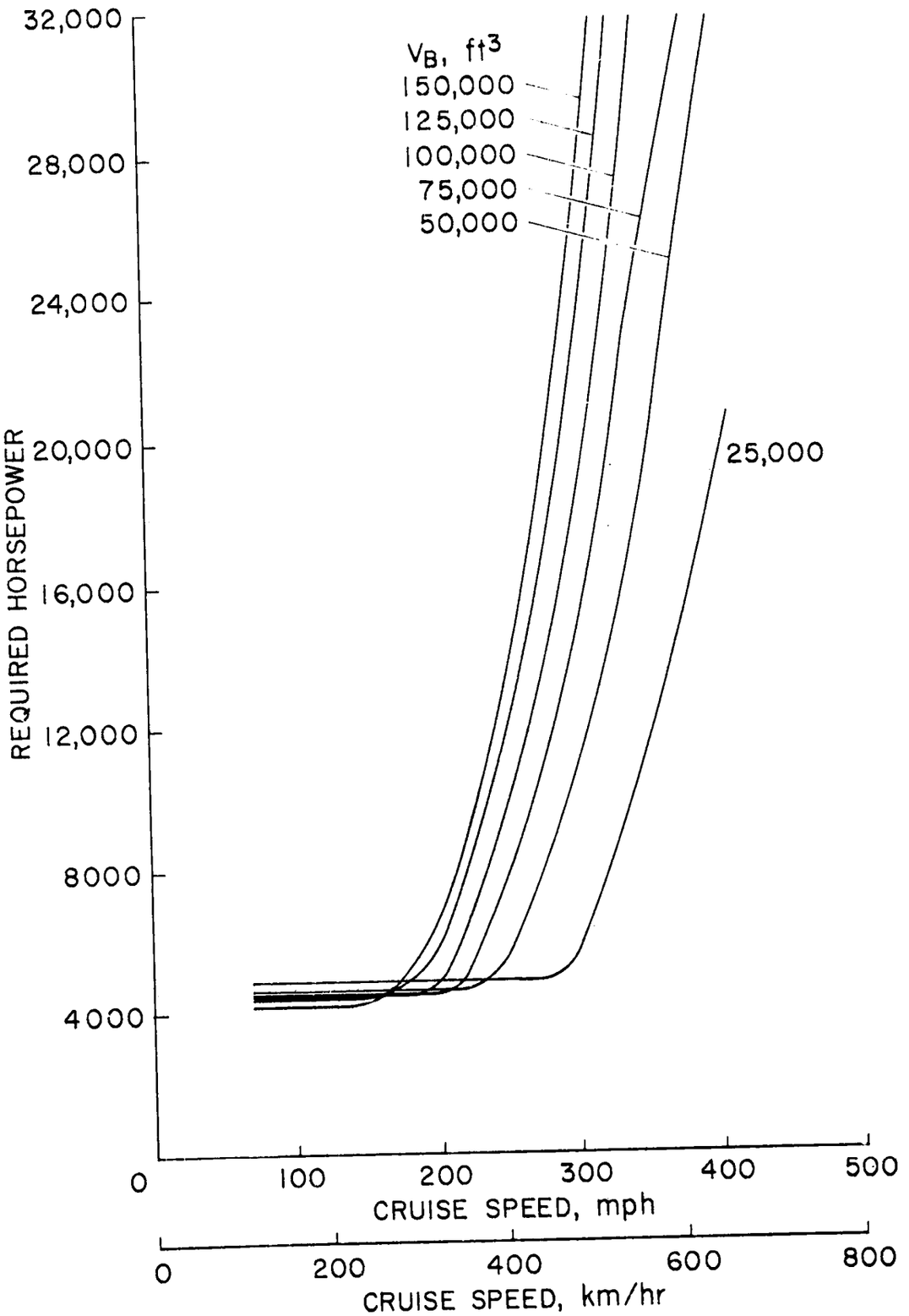

Figure 13.- Continued.

(b) C_L = .26

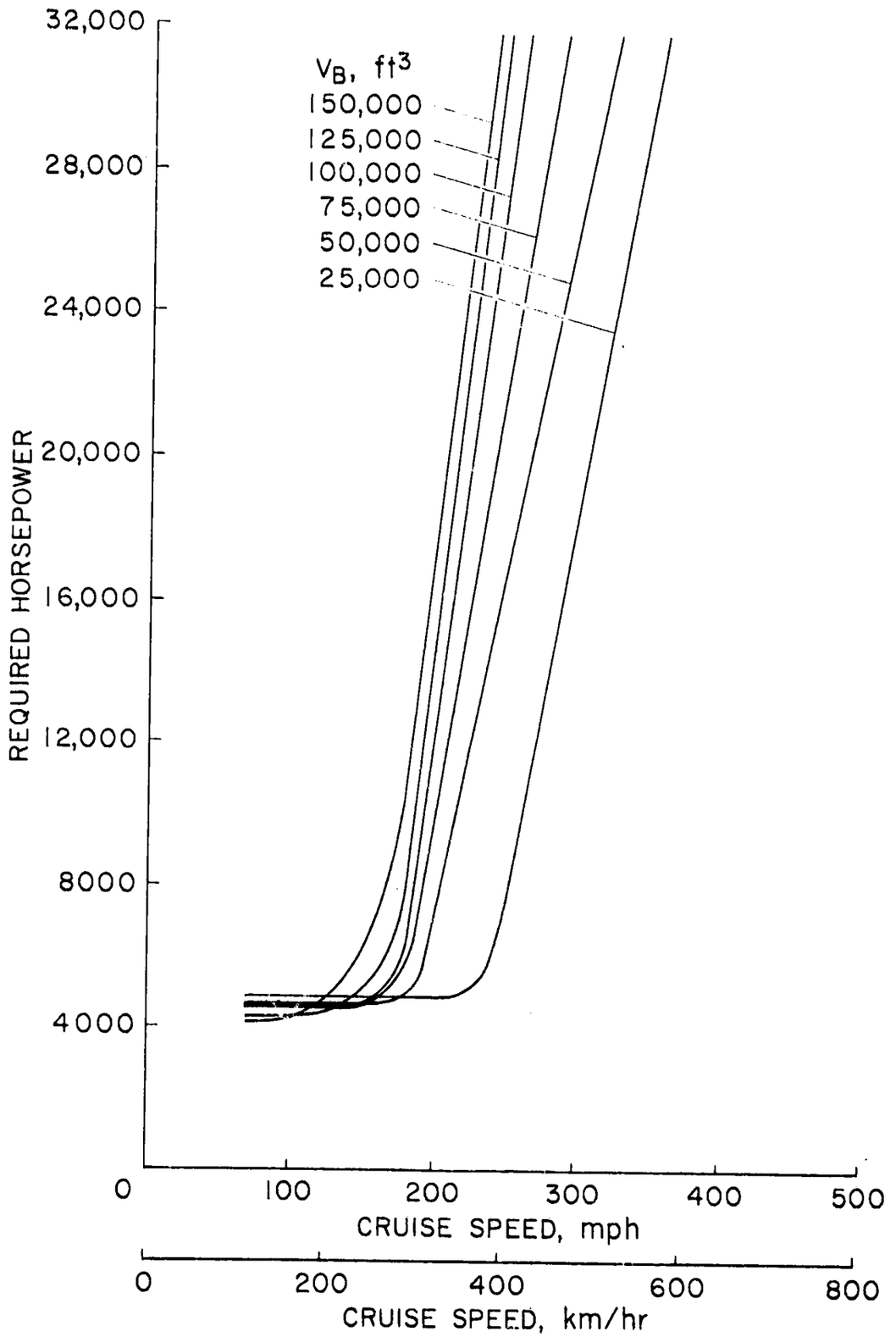

Figure 13.- Concluded. (c) C_L = .515

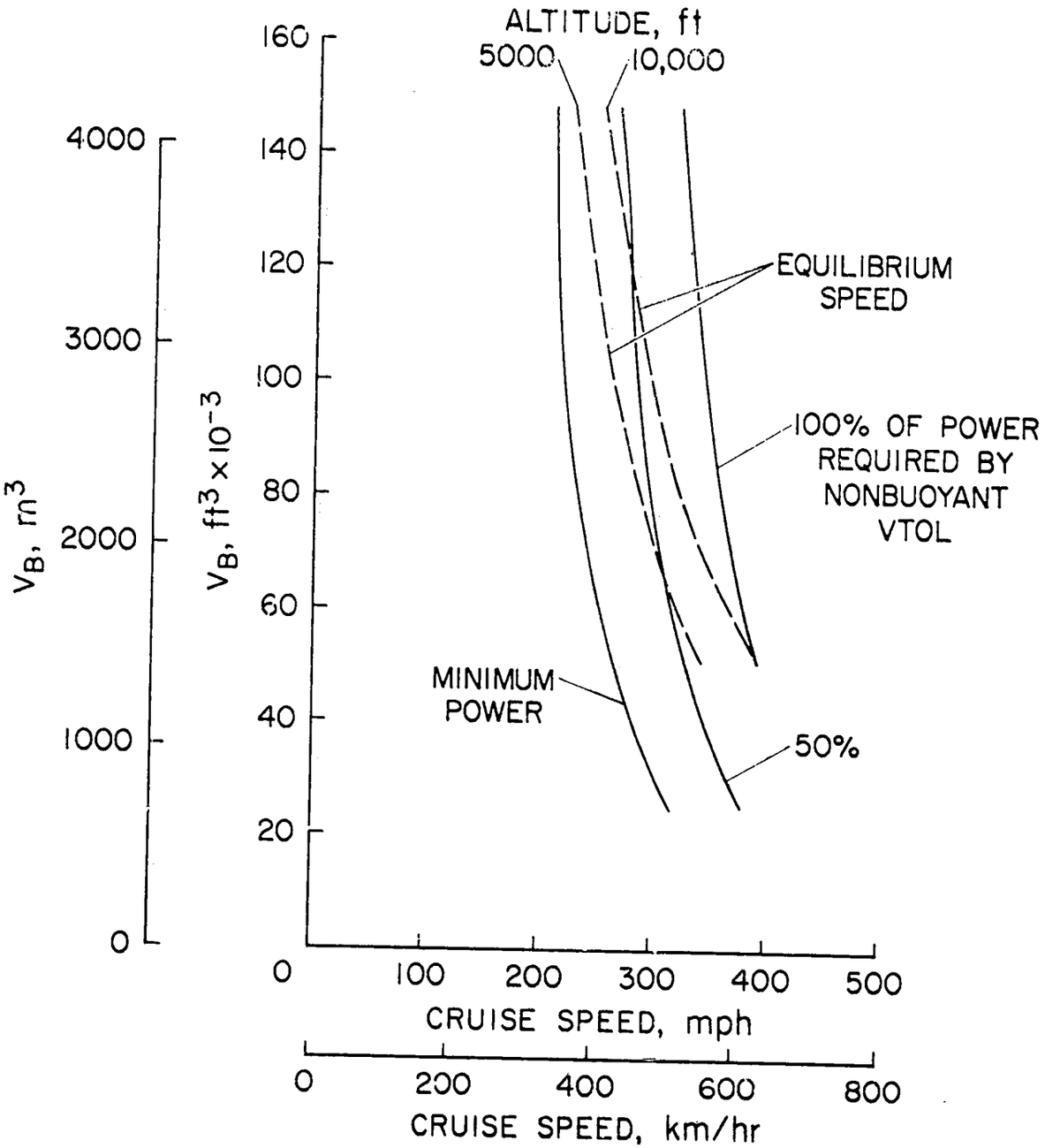

Figure 14.- Dynastat Power Limits.

(a) C_L = .12

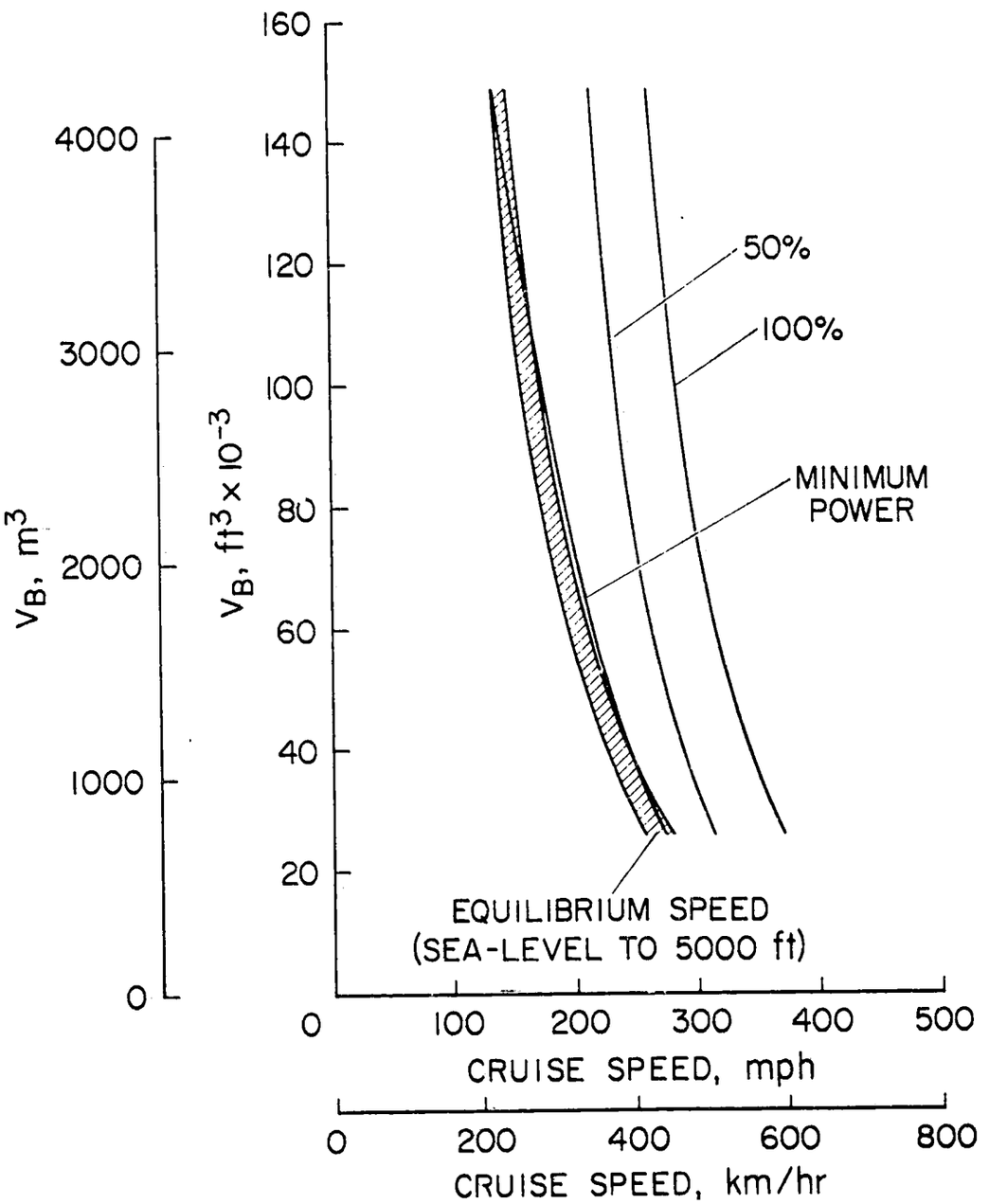

Figure 14.- Continued.

(b) C_L = .26

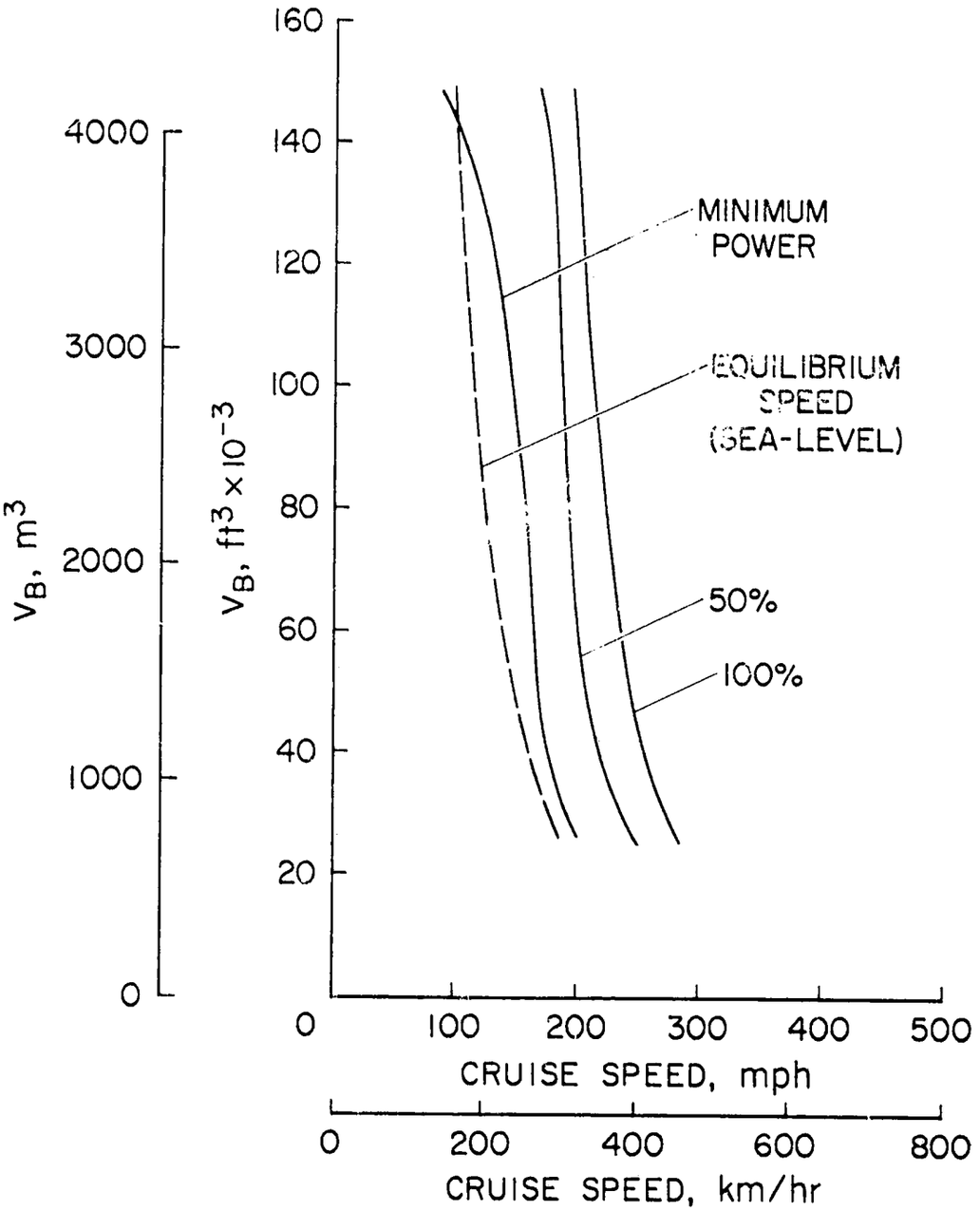

Figure 14.- Concluded.

(c) C_L = .515

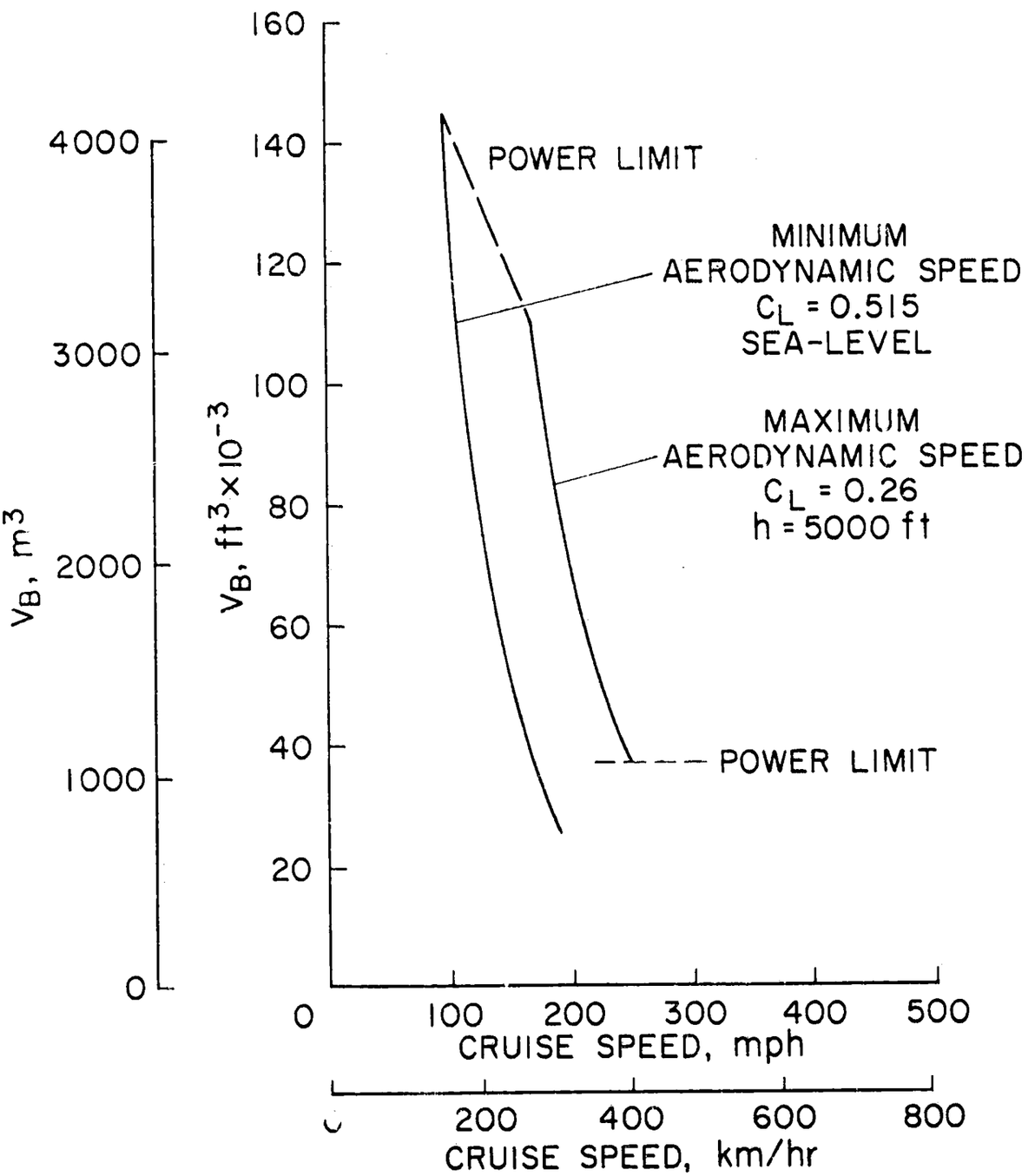

Figure 15.- Aerodynamic and Power Constraints.

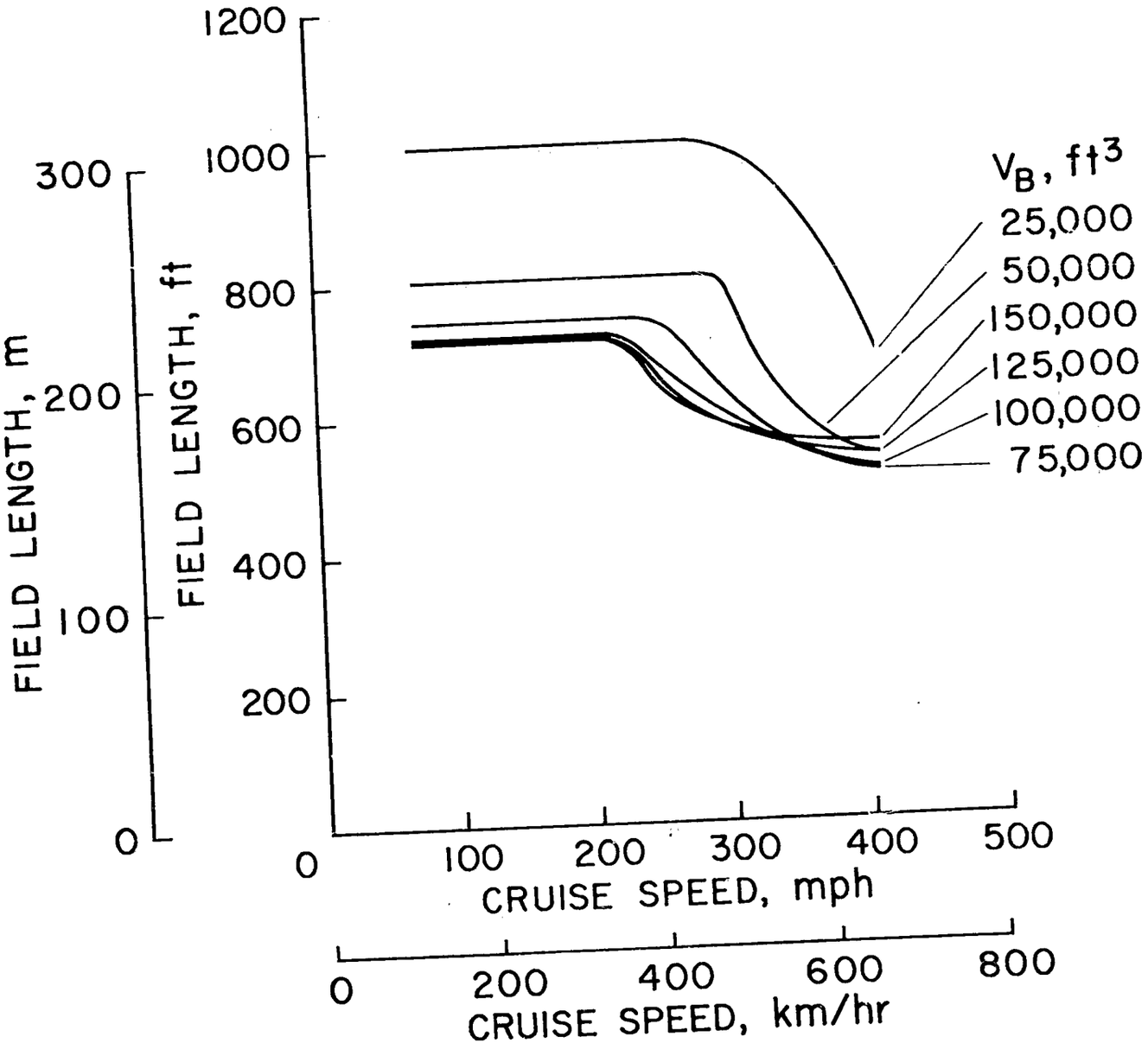

Figure 16.- Dynastat Field Length.

(a) C_L = .12

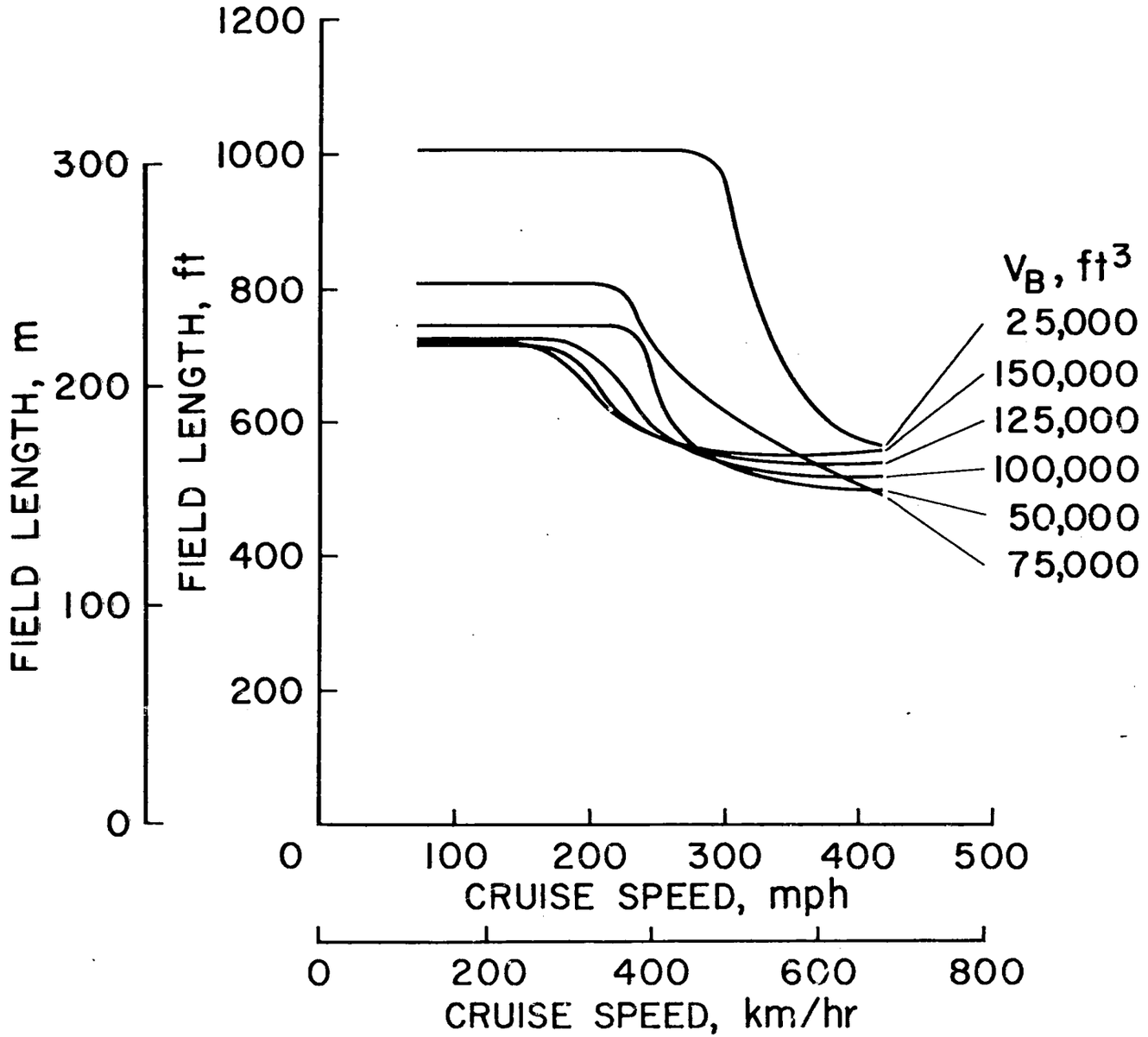

Figure 16.- Continued.

(b) C_L = .26

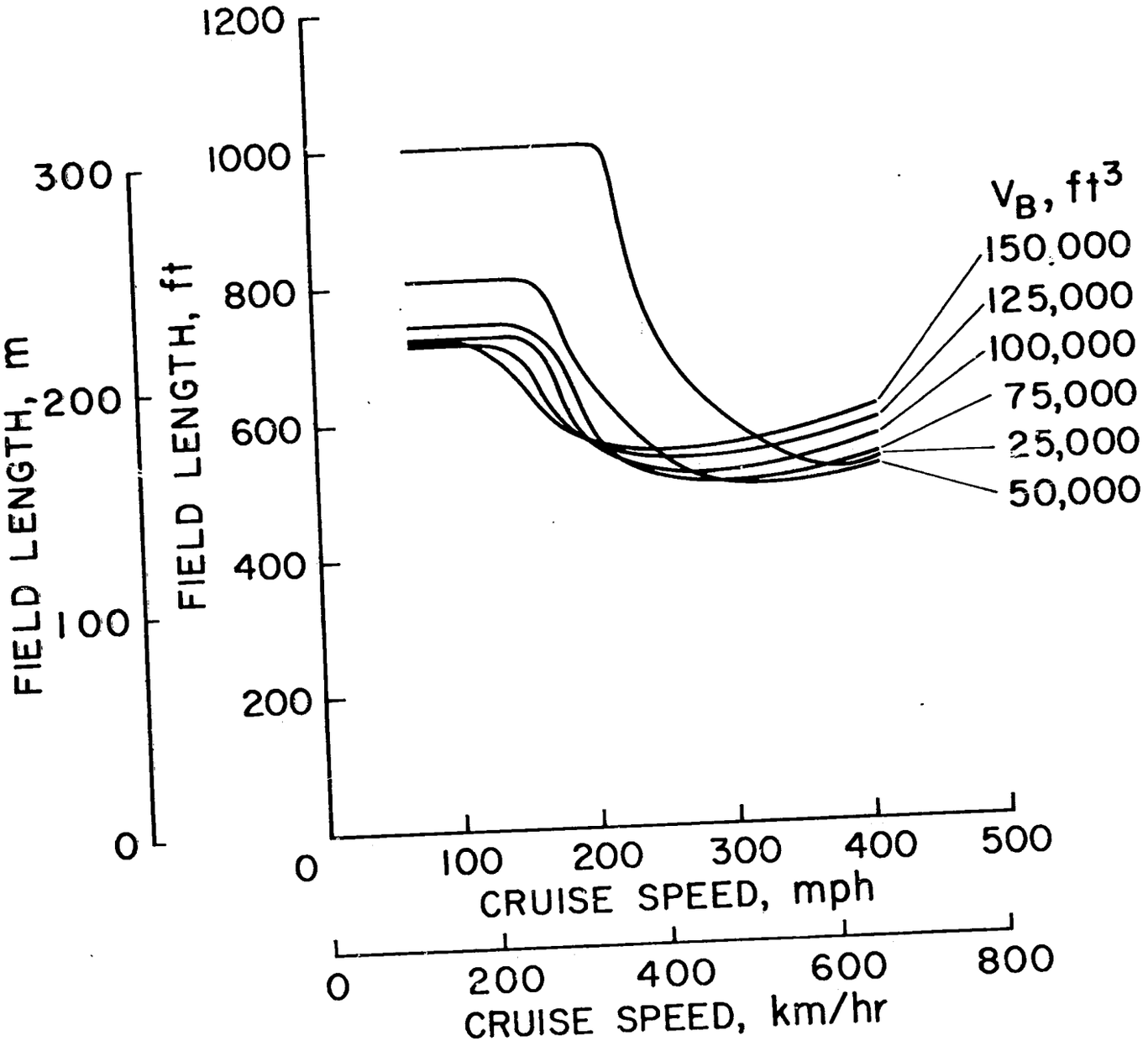

Figure 16.- Concluded.

(c) C_L = .515

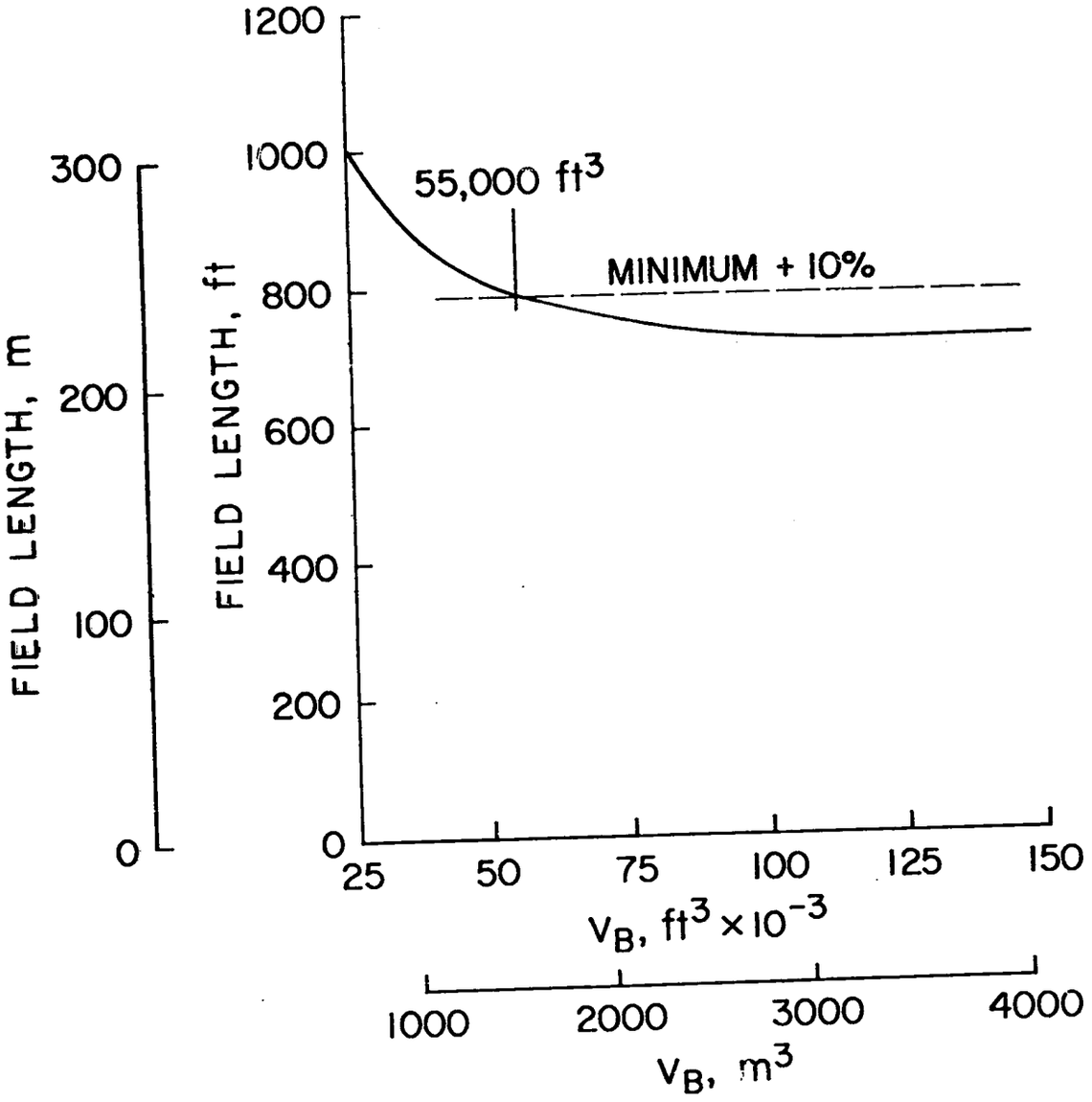

Figure 17.- Field Length Variation with Buoyant Volume for Dynastat Configuration.

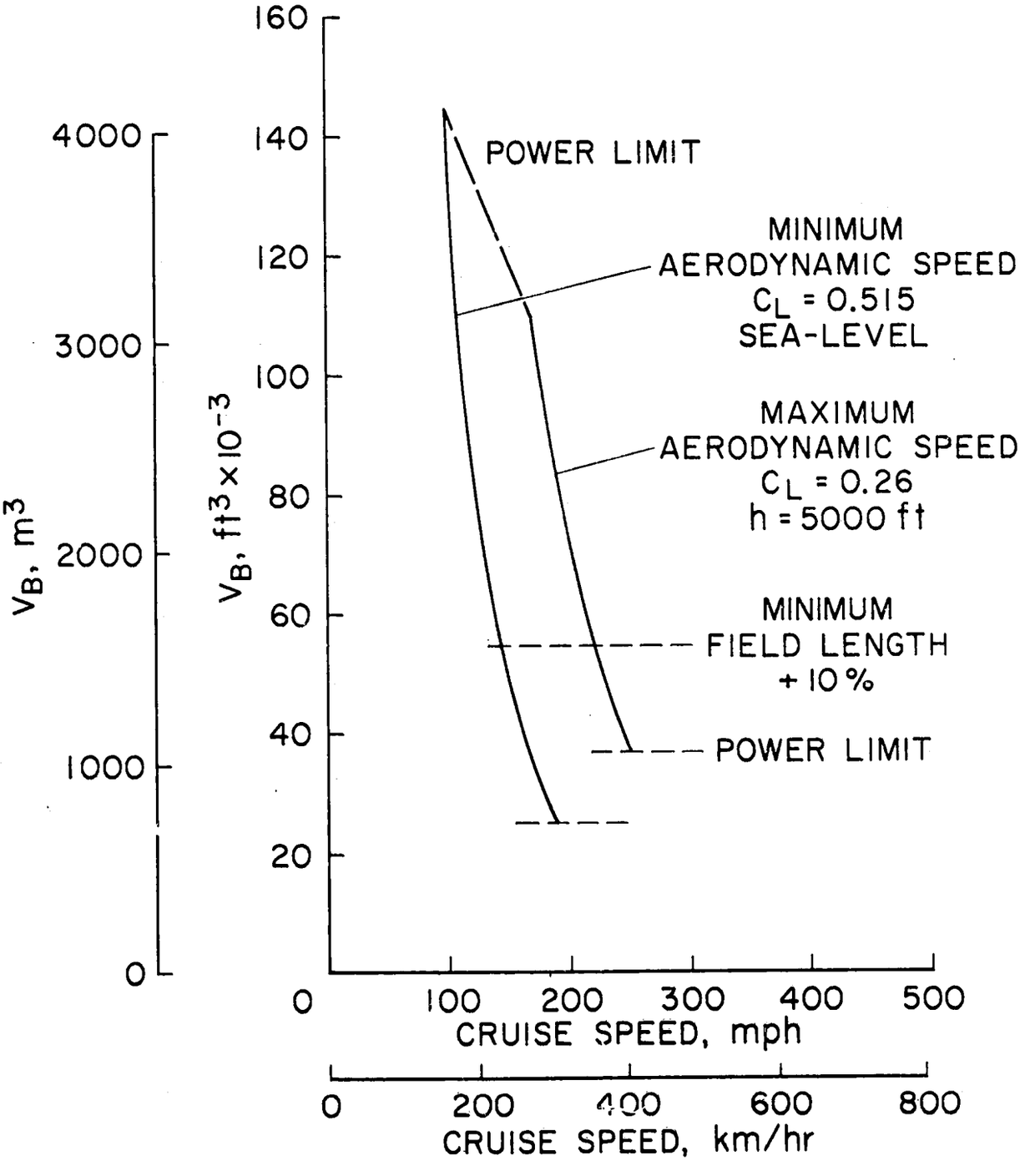

Figure 18.- Dynastat Design Constraints.

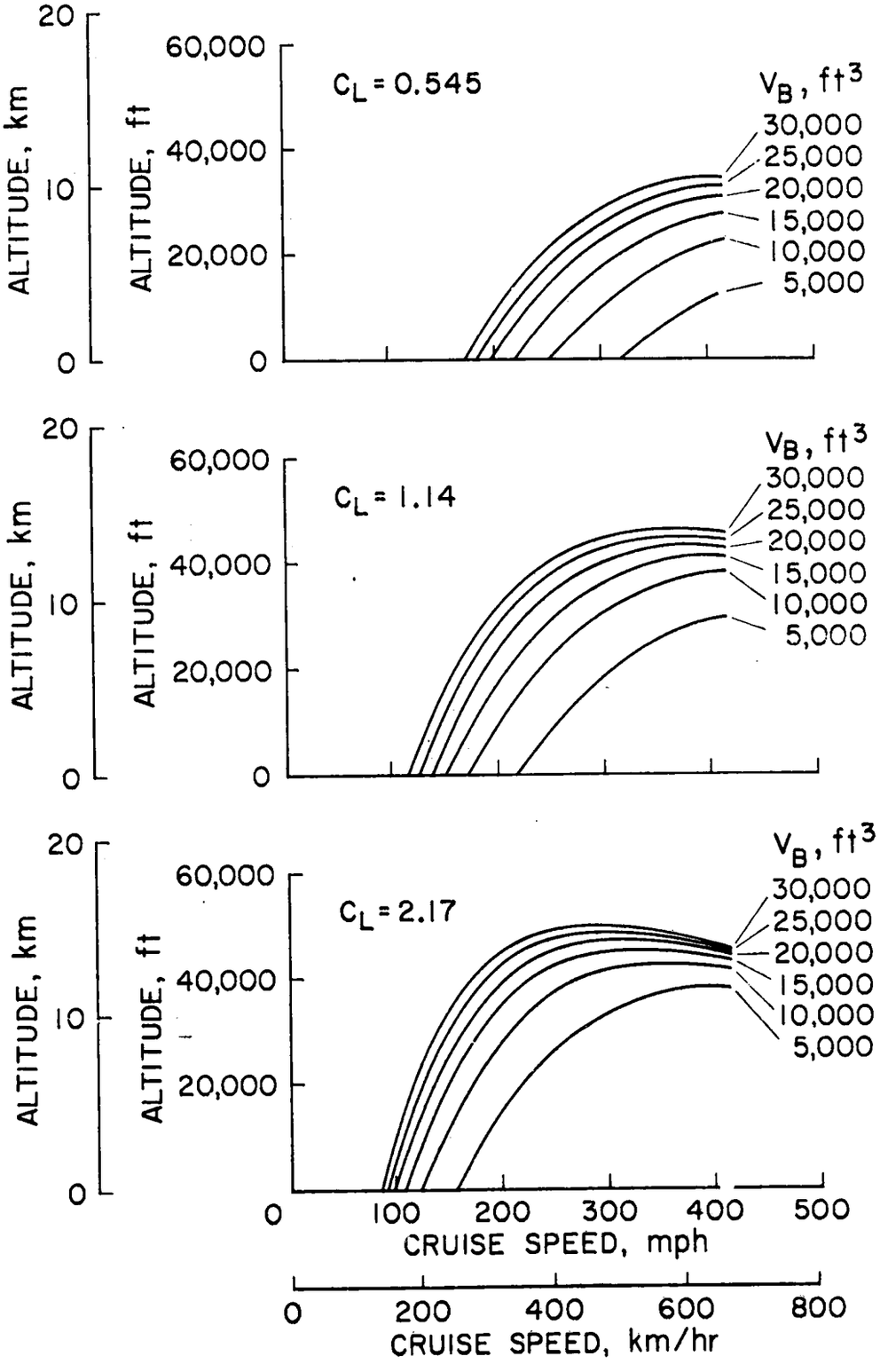

Figure 19.- Parawing Equilibrium Altitude.

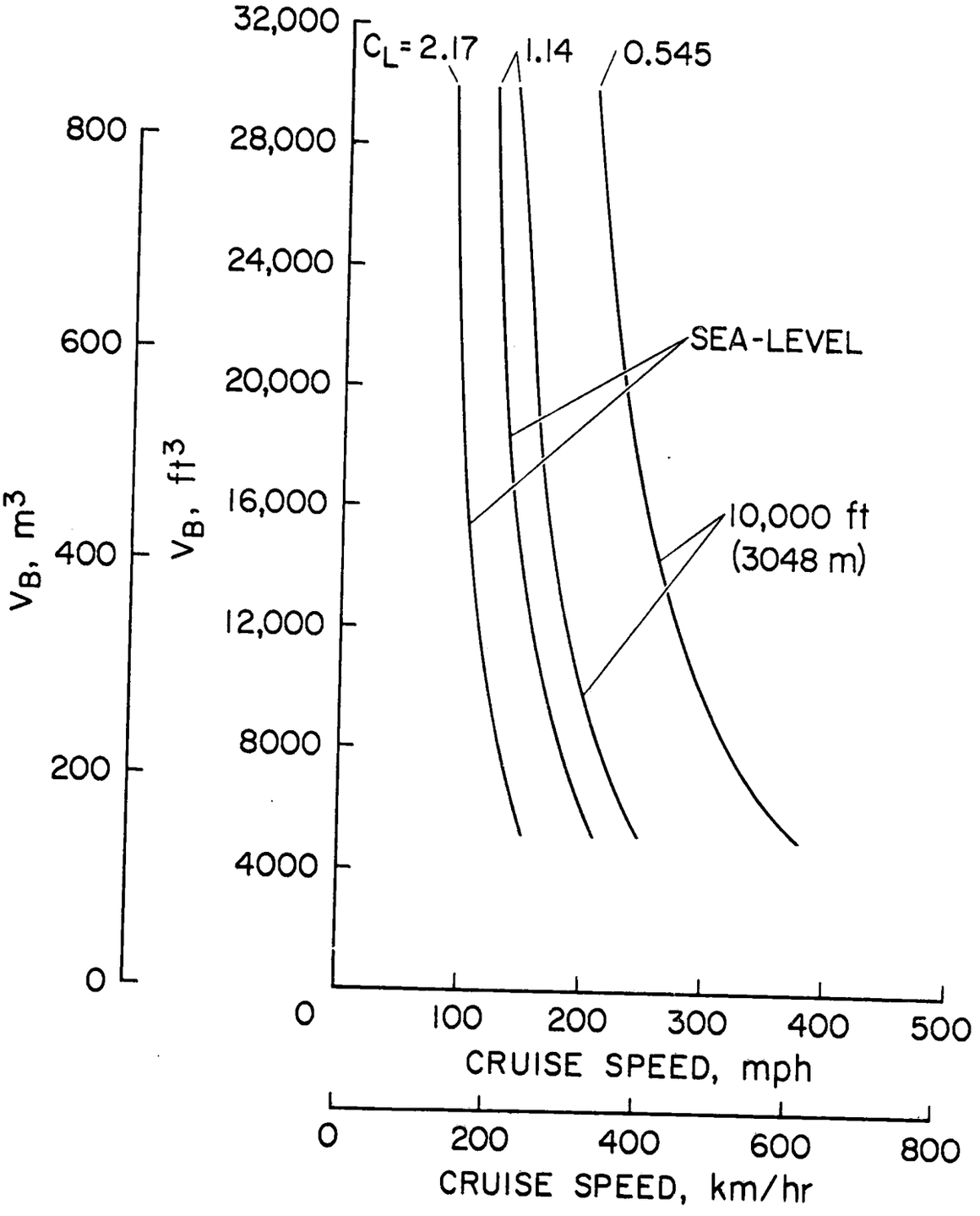

Figure 20.- Parawing Equilibrium Buoyancy.

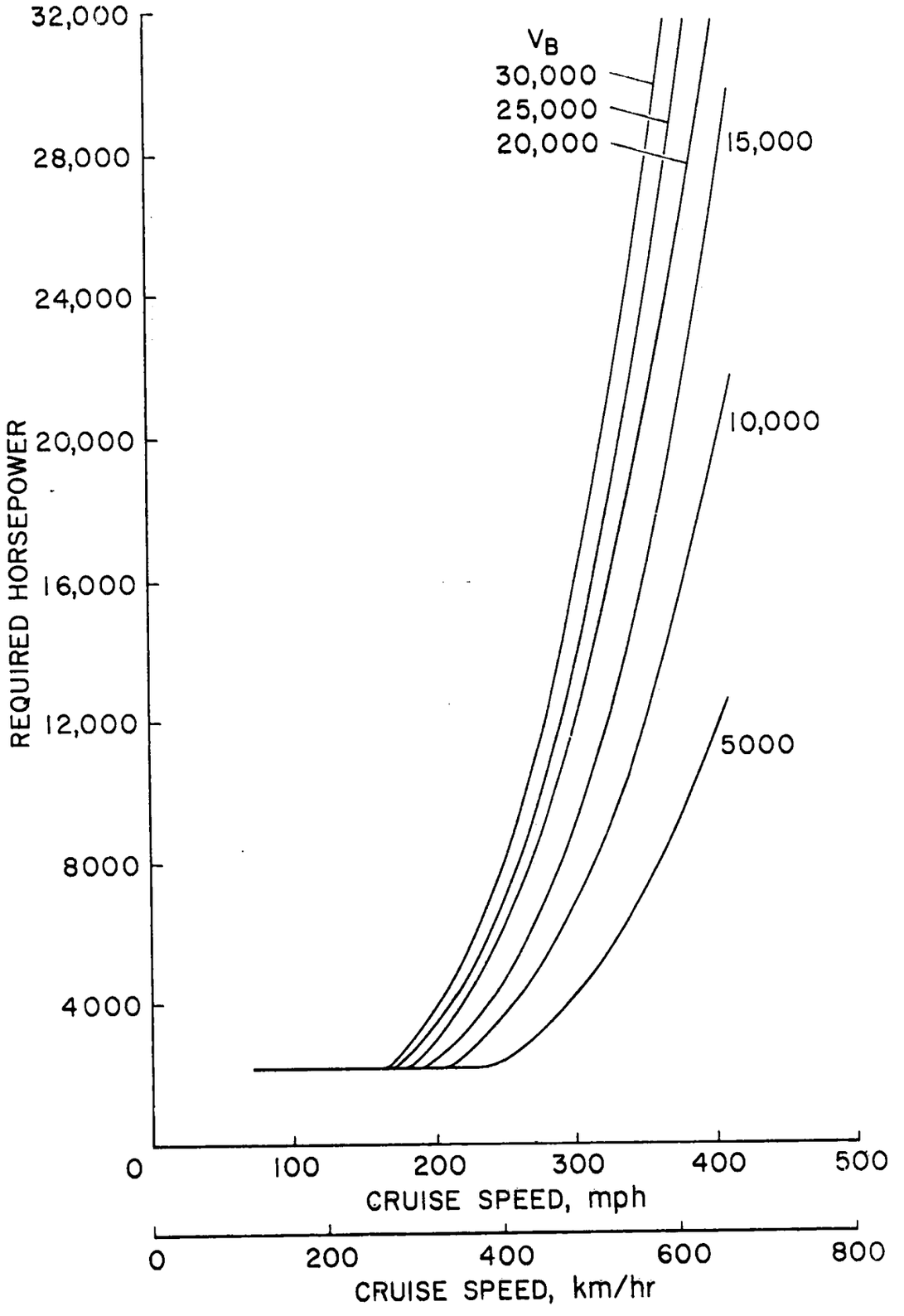

Figure 21.- Parawing Horsepower Requirements. (a) C_L = .545

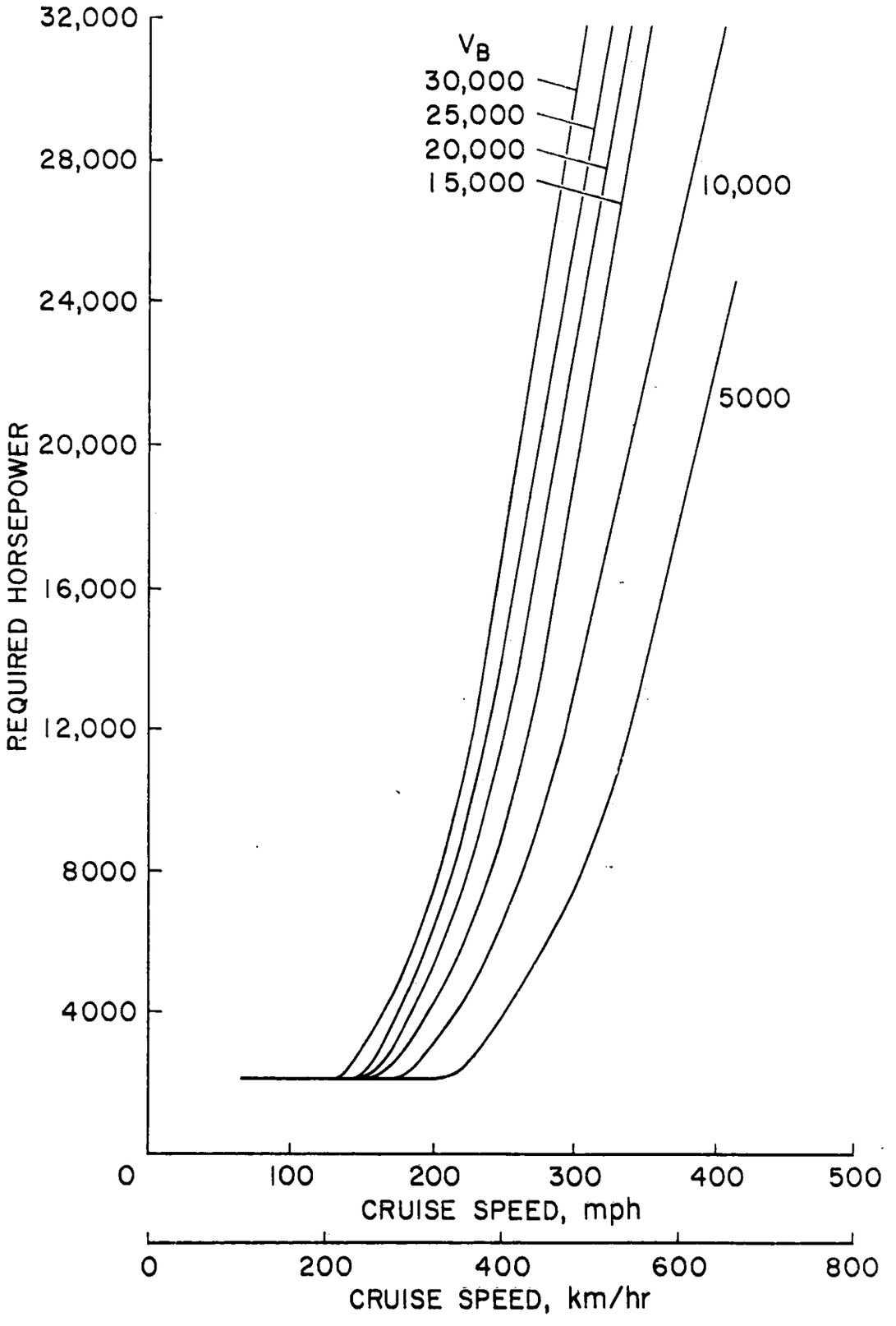

Figure 21.- Continued. (b) C_L = 1.14

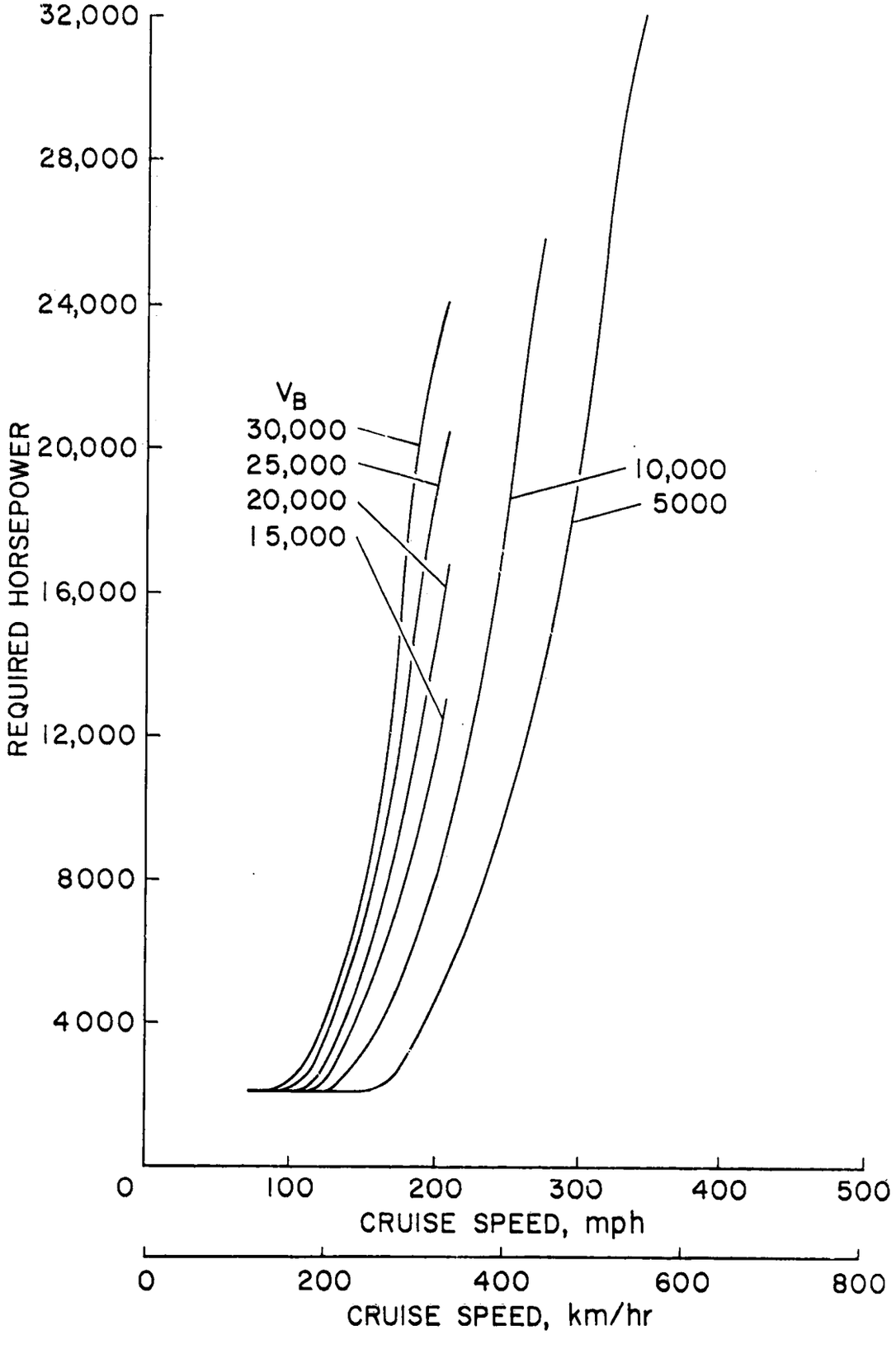

Figure 21.- Concluded.

(c) C_L = 2.17

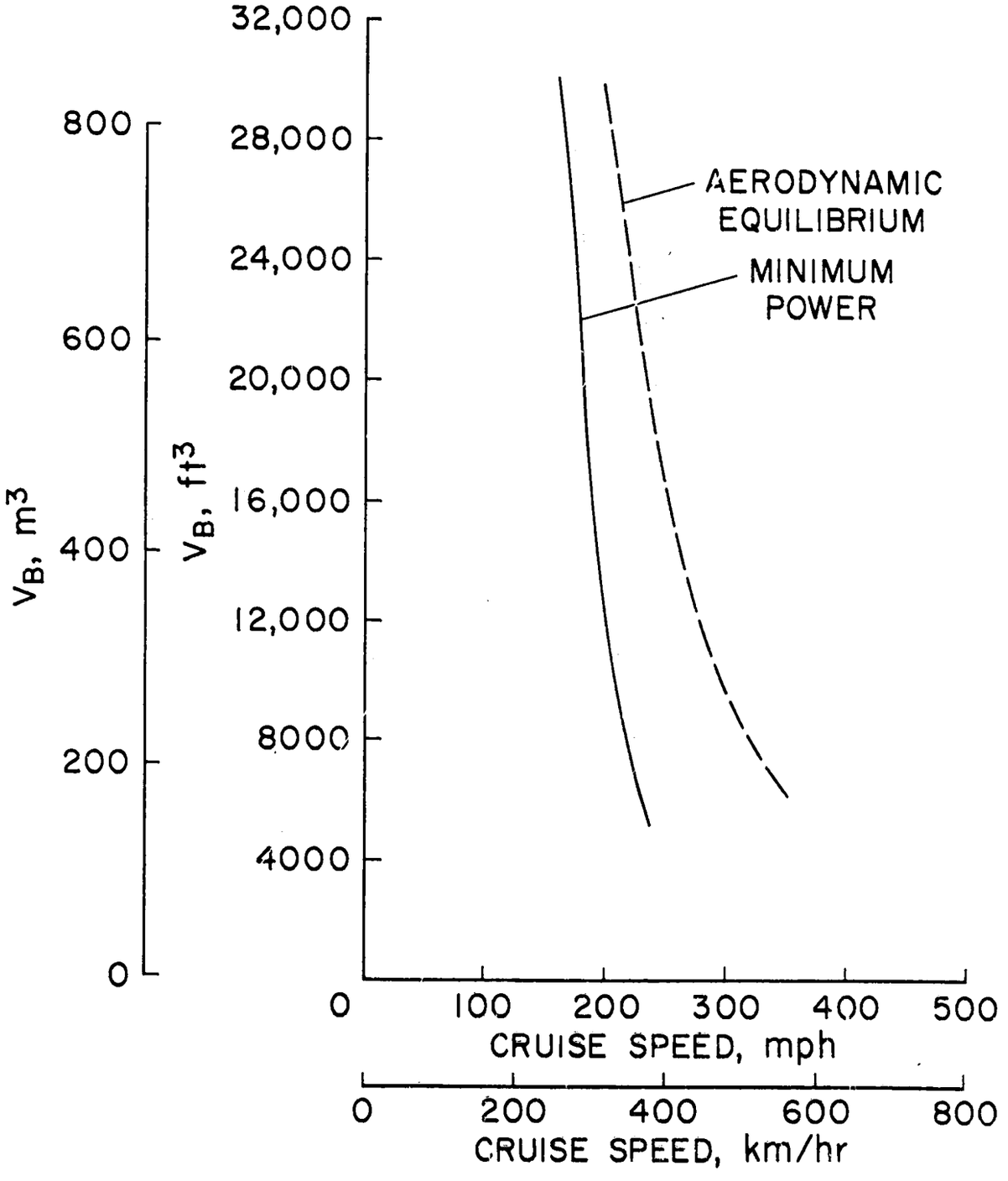

Figure 22.- Parawing Power Limits.

(a) C_L = .545

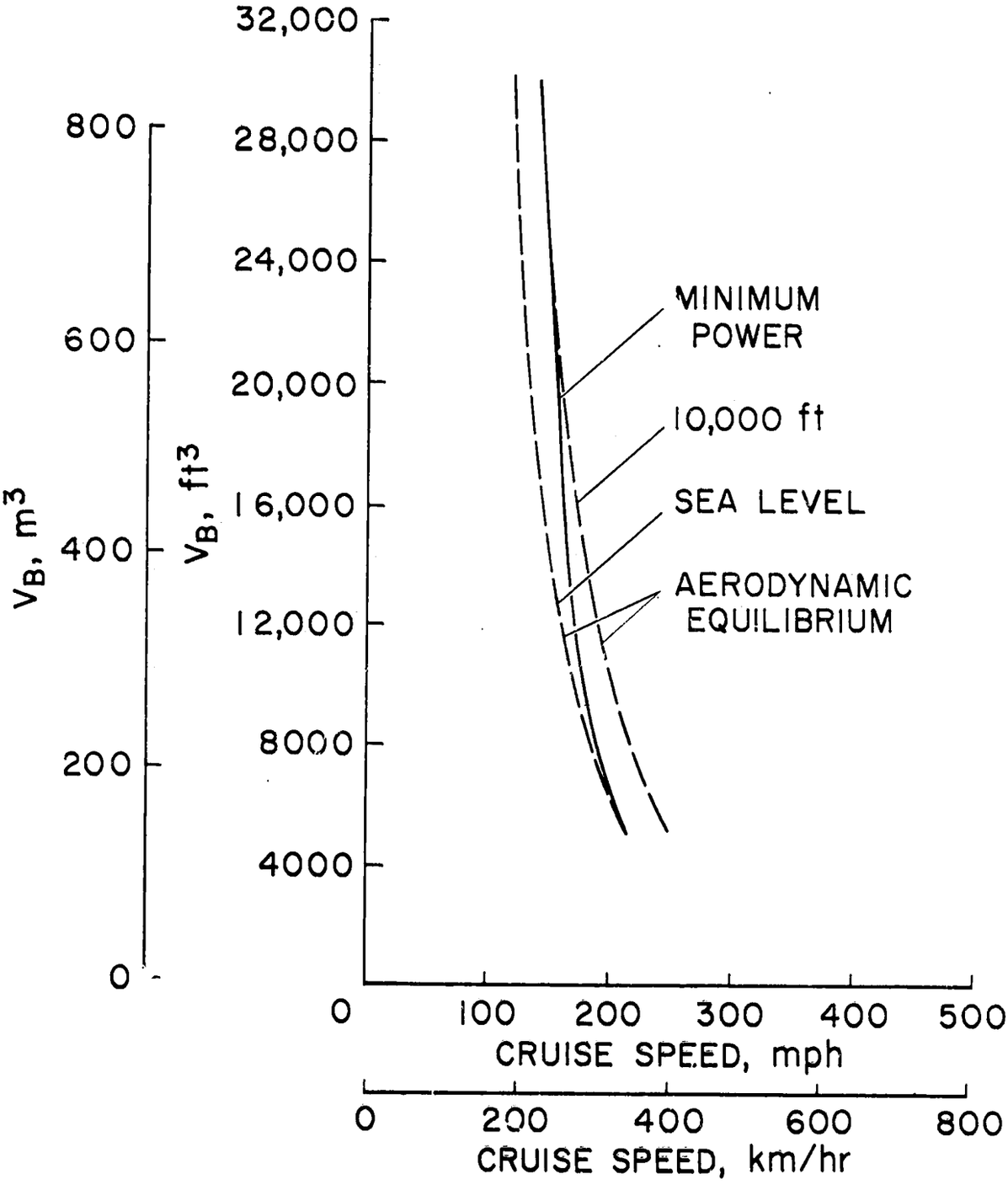

Figure 22.- Continued.

(b) C_L = 1.14

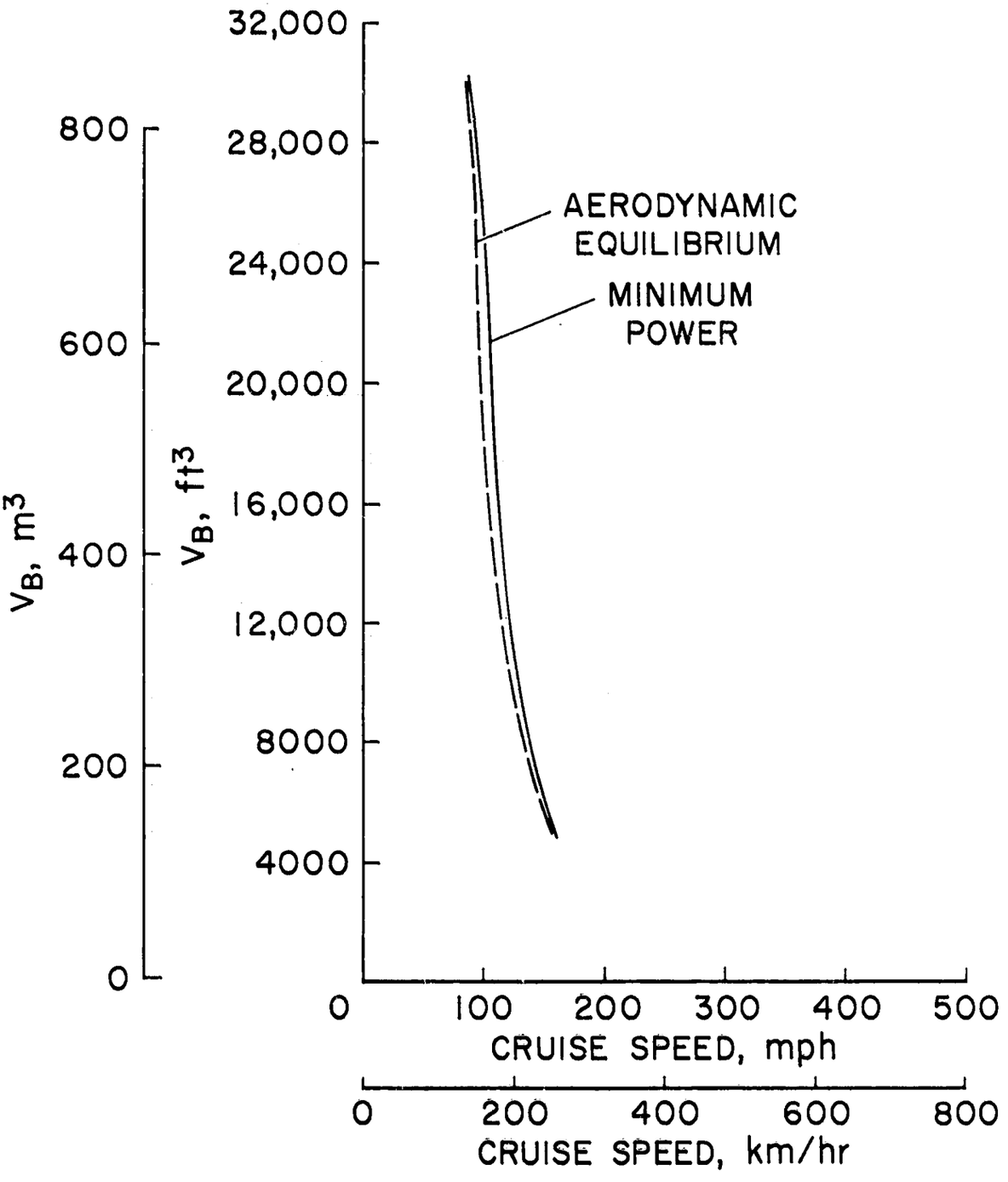

Figure 22.- Concluded.
(c) C_L = 2.17

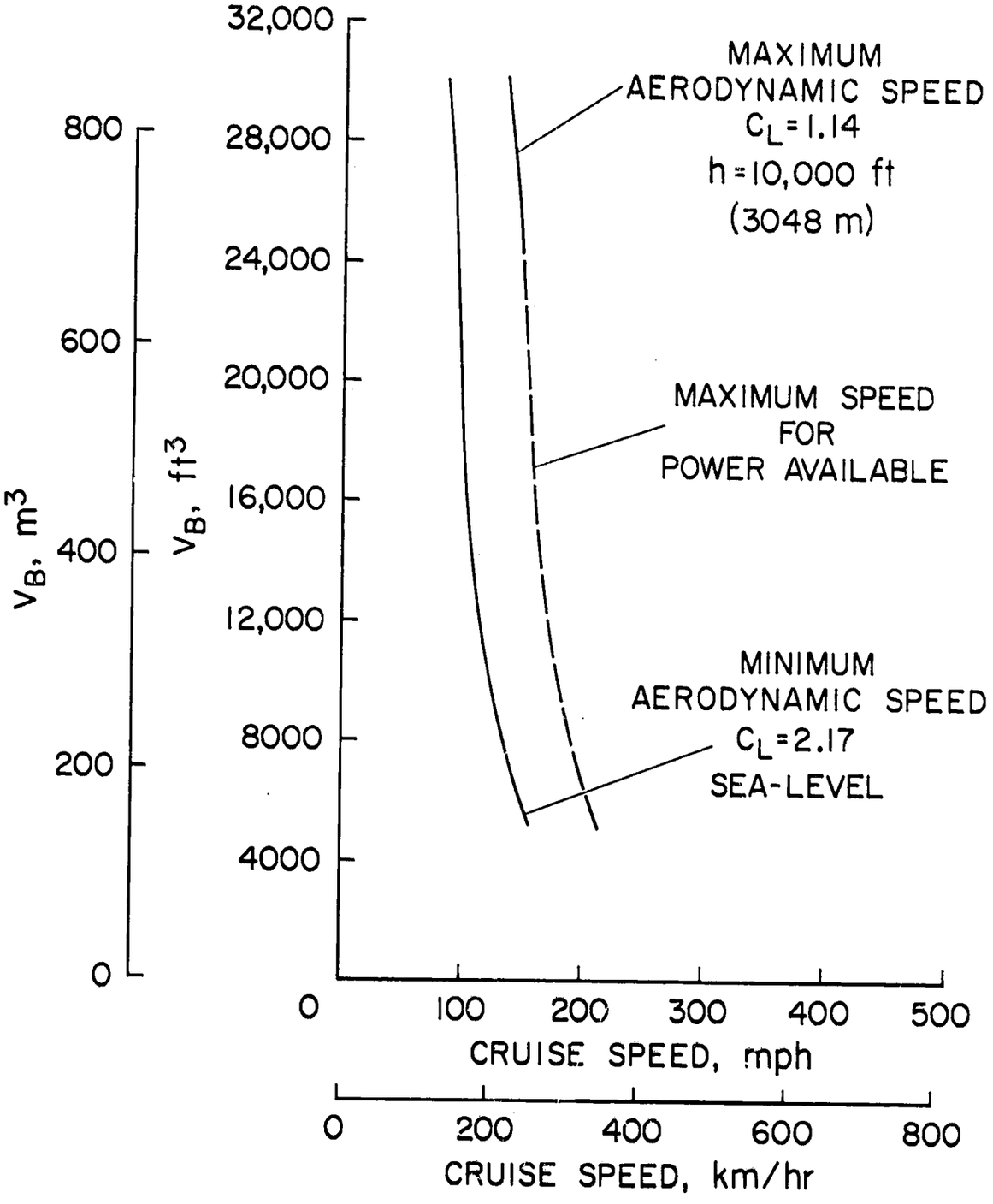

Figure 23.- Parawing Aerodynamic and Power Constraints.

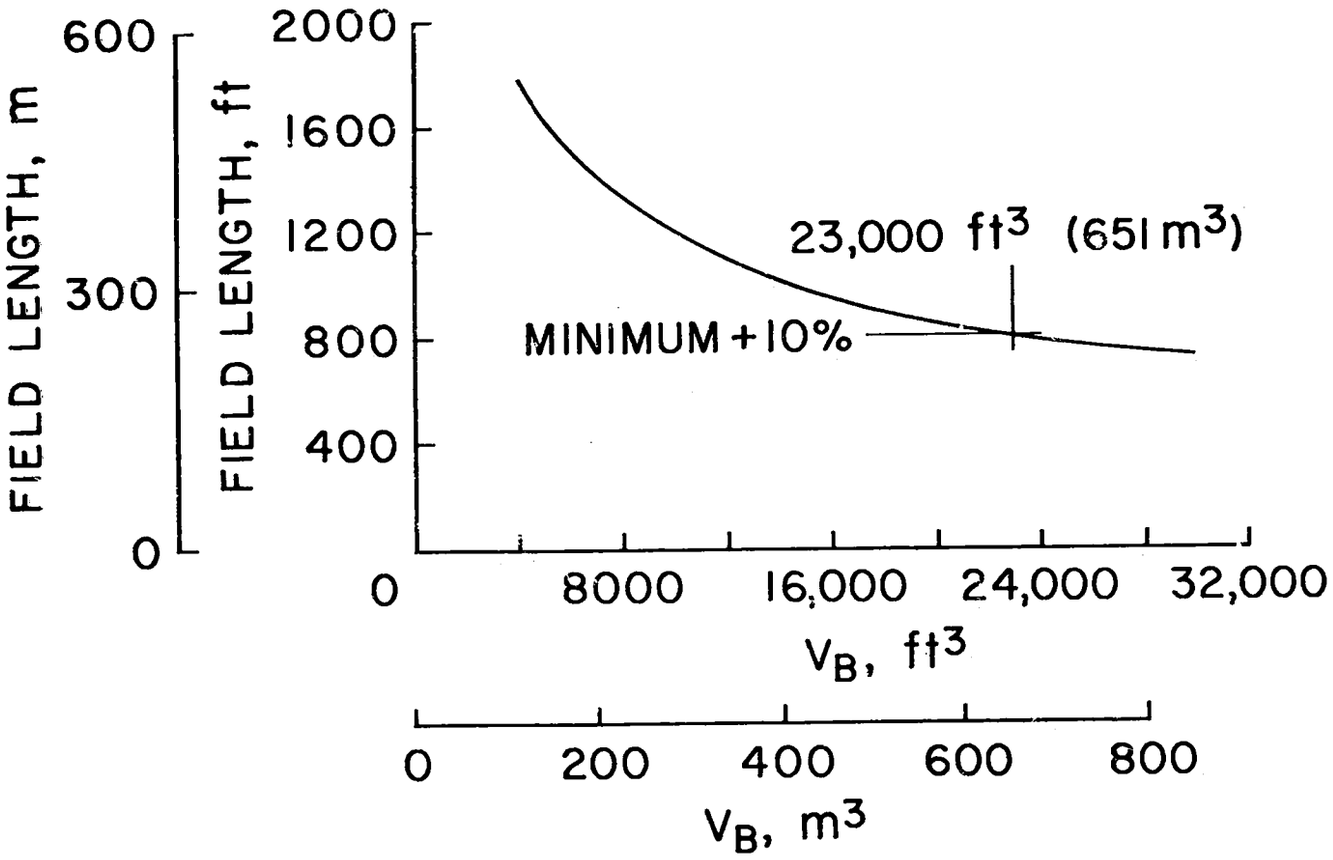

Figure 24.- Field Length Variation with Buoyant Volume for Parawing Configuration.

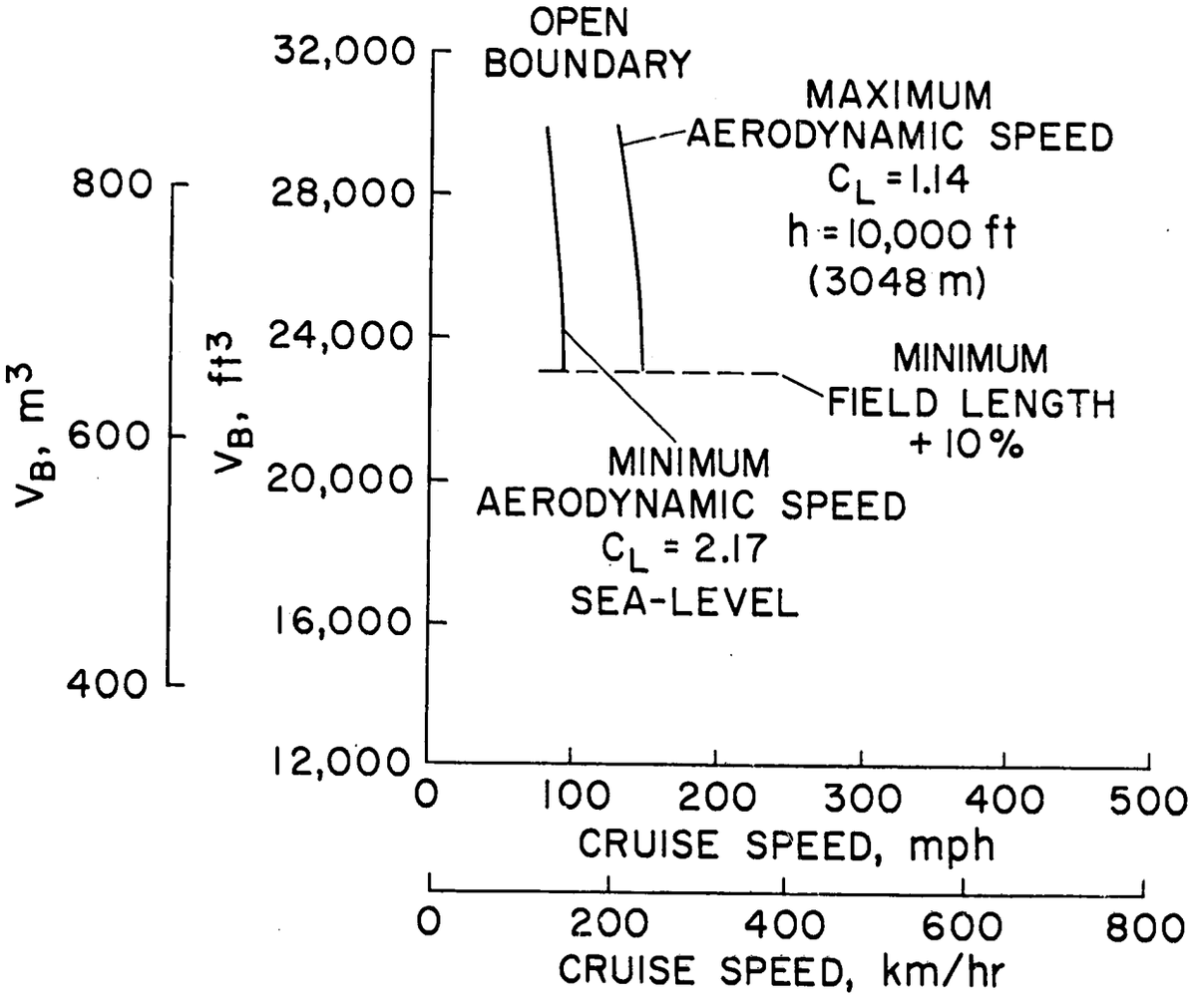

Figure 25.- Parawing Design Constraints.

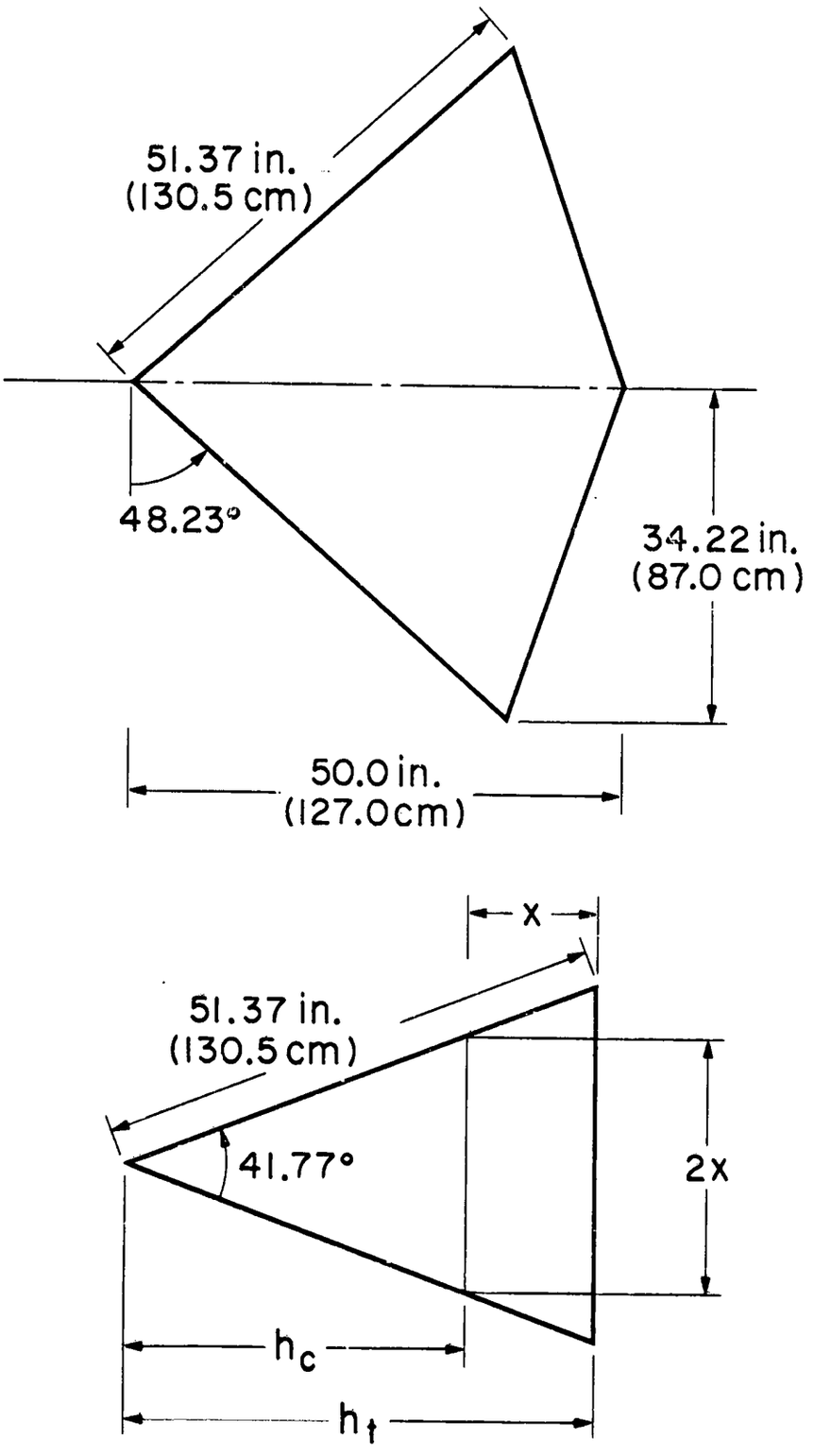

Figure 26.- Flat Planform Dimensions of Parawing Model with Geometric Representation of One Wing.